Jones-Wilkens-Lee (JWL) Equation of State with Afterburning

Leonard E Schwer
Schwer Engineering & Consulting Services 6122 Aaron Court Windsor CA 95492 USA
Len@Schwer.net

Abstract

The standard Jones-Wilkens-Lee equation-of-state for modeling detonation of high explosives was modified to allow inclusion of the additional energy associated with afterburning of fuel rich (oxygen poor) high explosives. Three options are available for including the additional afterburning energy:

1. *Constant energy rate addition*
2. *Linear energy rate addition*
3. *Miller Extension*

The performance of the afterburning equation of state is demonstrated via comparison with three experimental and numerical examples:

1. *LLNL HEAF Tests, Kuhl et al. (1998):*
2. *NCEL Tests, Keenan and Wager (1992):*
3. *Moby Dick Test, Miller & Guirguis (1993)*

Introduction

The detonation of a solid high explosive occurs in microseconds. If the explosive is not oxygen balanced, i.e. fuel rich lacking sufficient oxygen to burn all the reactants, the remaining reactants can burn and release their chemical energy at later times, on the order of milliseconds. This late burning and addition of energy is typically referred to as afterburning. The minimum requirements for this afterburning are sufficient external oxygen, i.e. from the surrounding environment, and sufficient temperature to maintain the chemical reaction.

When an explosive is detonated in a large volume of air, e.g. extremal free air detonations, any unreacted fuel is typically not converted to additional energy as the temperatures within the fireball quickly decrease and the chemical reaction is suppressed. However, when the same high explosive is detonated in an enclosed environment, i.e. within a chamber or room, the temperature, and pressure, remain well above ambient and may support the release of additional energy, if the reactants encounter sufficient additional oxygen. Some enhanced explosives are designed take advantage of late time afterburning via the inclusion of non-explosive particles, e.g. aluminum, that burn in the presence of elevated temperatures.

To include energy due to afterburning requires knowledge of the amount of energy that is released during afterburning, the time period over which the afterburning takes place and the rate of energy release over that time period.

Detonation product species and concentrations can be obtained using thermo-equilibrium codes such as Cheetah 2.0 (Fried et al, 1998). The amount of oxygen required to enable a full combustion process by reacting can be estimated by assuming a stoichiometric reaction of the reactants. As an example, Cheetah predicts about 4.5 MJ/kg for TNT. The theoretical energy release from oxidation of all the detonation products is 10.01 MJ/kg-for TNT. This gives a ratio of the total combustion energy (detonation + afterburning) to the detonation energy of 3.23 (Erdi, et al 2012).

For detonation in enclosed spaces, the approximate time the afterburning starts is when a shock wave reflects from a wall and interacts with the detonation products. It is assumed this reflected shock causes sufficient mixing of external oxygen with the available reactants in the detonation products. The afterburning terminates when the temperature drops below that needed to sustain the reaction or the available external oxygen is consumed.

Two simple energy rate assumptions are constant and linearly increasing. A slightly more complex assumption is due to Miller (1996) and usually referred to as Miller's Extension for afterburn energy. Beyond these simple engineering models for energy release rate, there exist sophisticated thermodynamic models, see for example Kuhl et al. (2003)

Modified JWL Equation-of-State: *EOS_JWL_AFTERBURN (EOS13)

The JWL_AFTERBURN equation of state modifies the traditional JWL equation of state with the addition of afterburn energy Q

$$p = A\left(1-\frac{\omega}{R_1 V}\right)e^{-R_1 V} + B\left(1-\frac{\omega}{R_2 V}\right)e^{-R_2 V} + \frac{\omega\left(E+Q\right)}{V}$$

The traditional JWL parameters are A, B, R_1, R_2, ω and E_0. The additional parameters needed are the afterburn energy, Q , the start and end times for adding the afterburn energy, and the rate at which the afterburn energy is add to the calculation.

The present implementation adds afterburn energy to the equation of state in one of three ways, via the input parameter:

QOPT	=0	No afterburn energy (standard JWL EOS)
	=1	Constant rate afterburn energy between T_1 *and* T_2
	=2	Linearly increasing rate afterburn energy between T_1 *and* T_2
	=3	Miller's Extension afterburn energy

For Miller's Extension the afterburn energy is added via a time dependent growth term

$$\frac{d\lambda}{dt} = a\left(1-\lambda\right)^m P^n$$
$$Q = \lambda Q_0$$

A caution about Miller Extension parameters obtained from the literature. It is often recommended that a unit system of gram, centimeter, microsecond be used when a model includes high explosive. In this consistent unit system, pressure is in Mbar.

Many of the published parameters for Miller's Extension use Mbar for the unit of pressure. To allow users could convert their units to Mbar for the Miller's Extension calculation, the above rate equation was implemented as

$$\frac{d\lambda}{dt} = a\left(1-\lambda\right)^m \left(P_{con}P\right)^n$$

Here the new term P_{con} serves to convert the user units of pressure to Mbar. For example, input pressure units are MPa, then the conversion to Mbar is to divide MPa by 10^5 or $P_{con} = 10^{-5}$. Also note, the energy release constant a has units of 1/time, so if values from the literature are to be used, the input value of a should be adjusted to be consistent with the user's time units.

Simulation of LLNL HEAF Tests

Kuhl et al. (1998) conducted closed cylindrical chamber tests using 0.8kg of TNT to study the effects of afterburning. The test was conducted in an air filled chamber and then repeated with the chamber filled with nitrogen, to inhibit afterburning of the TNT detonation products. The pressure histories were measured at five gauge locations. Subsequently, Edri et al. (2013) used AUTODYN to simulate the tests and reported the pressure history at one location.

This section focuses on simulating the LLNL HEAF tests using the newly implemented LS-DYNA® afterburning JWL equation-of-state. First the non-afterburning data is used to examine some of the ancillary computational parameters associated with detonation and air blast simulations.

LLNL HEAF Tests

The tests were conducted at the Lawrence Livermore National Laboratory (LLNL) High Explosion Application Facility (HEAF) in a closed cylindrical chamber. The following chamber, charge and diagnostics descriptions are from Kuhl et al. (1998):

> The chamber was constructed as a cylindrical stainless steel tank (inner diameter D=2.38m and length L=4m) with a volume of V= 16.64m^3.
>
> The explosive charge consisted of 800g TNT, a 50g LX-10 booster, and a 25g SE-I detonator, with a total mass of 875g. The TNT was pressed to a density of 1.63g/cm^3, in the form of cylindrical plugs (5cm in diameter and 9.1cm long); three such plugs were then glued together with Eastman-910 adhesive, to form the final 800g TNT charge (diameter d=5 cm and length L=27.34cm).
>
> The primary diagnostic consisted of five quartz pressure transducers (PCB Piezotronics Inc. Model 102A), mounted in fixtures on the side wall of the test chamber at

approximately 130cm distance from the charge. Also, beaded thermal couples (Omega model CHAL-022) were used to estimate the temperature of the post-explosion gases.

Unfortunately, the figure (Figure 2 in Kuhl et al.) depicting the chamber interior, and possibly gauge locations, is not legible in the copy of the report that is available via the internet. However, since the quantity of interest is the final pressure in the tank, the exact location of the gauges in not required, as all gauges should have the same final pressure. Indeed, this is the case for the reported three pressure gauges from the TNT in air test, Figure 5 in Kuhl et al.; only one pressure gauge history data was reported for the TNT in nitrogen test, Figure 4 in Kuhl et al.

LLNL HEAF Test Model

A Multi-Material ALE (MM-ALE) axisymmetric model of the half-length cylinder was created using uniform 5 and 2.5mm meshes, see Figure 1. All four exterior edges of the mesh were constrained from normal displacement. Since the density of air and nitrogen are quite similar, i.e. 1.25 and 1.29 km/m^3, respectively, and their ratio of specific heats are identical, i.e. $\gamma = 1.4$ the simulated tank was filled with air modeled as an ideal gas for both the air and nitrogen cases; the simple afterburn model does not include chemical reactions. The TNT charge was included in the model using the LS-DYNA keyword *INITIAL_VOLUME_FRACTION_GEOMETRY to fill the corresponding MM-ALE region. For the 5mm mesh spacing there are 5 cells across the radius of the charge, which is less than the rule-of-thumb minimum 10 cells; the 2.5mm mesh discretization, with 10 cells across the radius, the two mesh results are compared to assess one of the modeling parameters. The equivalent 875g TNT charge was modeled using the JWL equation-of-state with parameters obtained from Dobratz & Crawford (1985) and was center detonated.

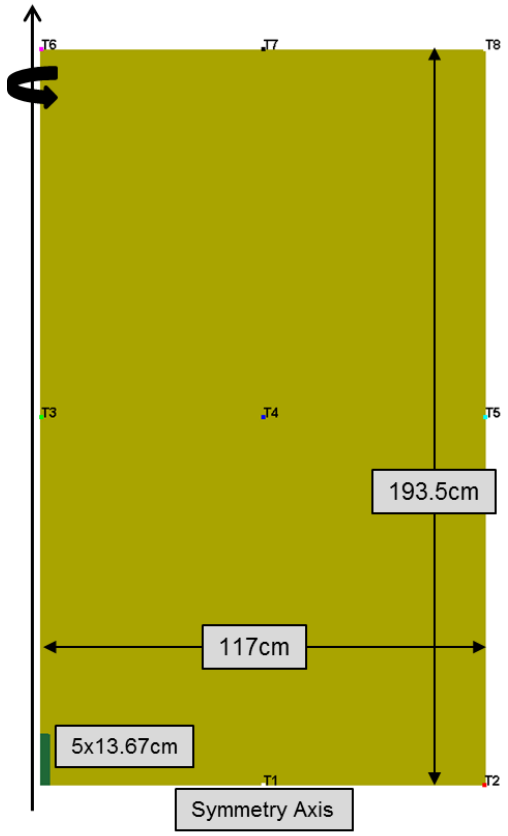

Figure 1 Axisymmetric half-length model of the LLNL HEAF cylinder with locations of 8 tracer particles indicated and charge (green) in lower left corner.

Simulation Results

Before attempting the afterburning simulation, the above described model was used to simulate the non-afterburning case. Figure 2 is a crude hand digitization[1] of Figure 4 in Kuhl et al. depicting the pressure histories for TNT detonated in the air and nitrogen filled chamber. Unfortunately, this nitrogen filled chamber pressure history is the only gauge measurement for the non-afterburning pressure history. Figure 7 in Kuhl et al., here reproduced as Figure 3, also shows a comparison of the pressure histories in air and nitrogen, but these are moving (time) averaged plots using an averaging window of 7.5ms. From this time averaged plot Kuhl et al estimated final chamber pressures of 2.8 bar (280kPa) in air and about 0.85 bar (85kPa) in nitrogen.

[1] The digitized data was kindly provided by Idan Edri of the Technion; primary author of Edri et al (2013).

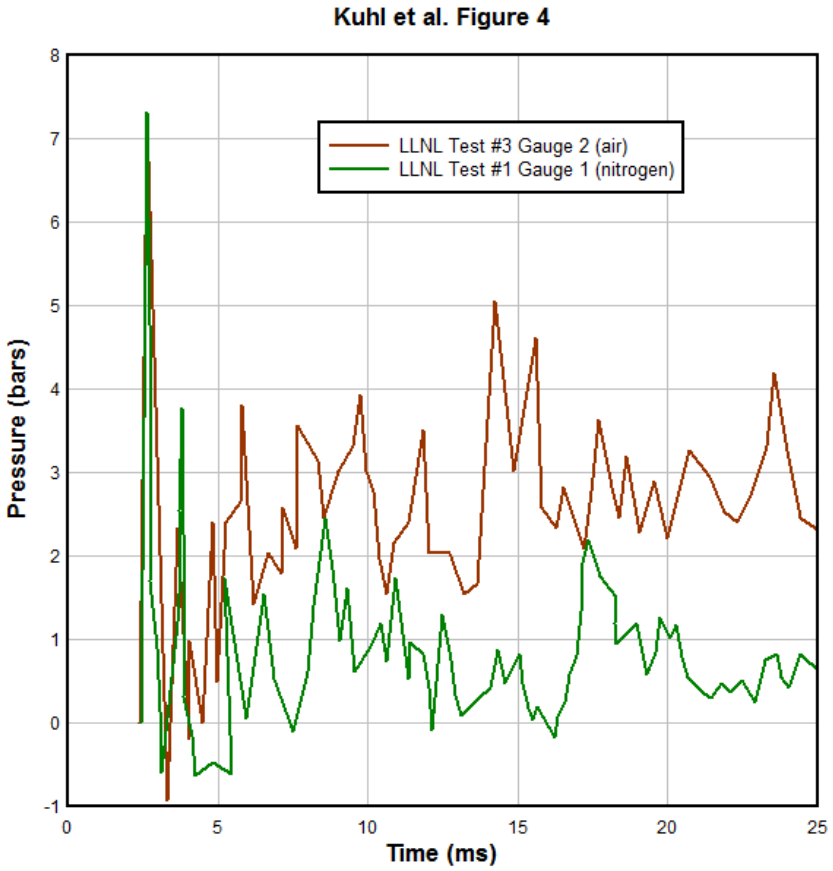

Figure 2 Hand digitization of Figure 4 in Kuhl et al. showing pressure histories for TNT detonation in air and nitrogen filled chambers.

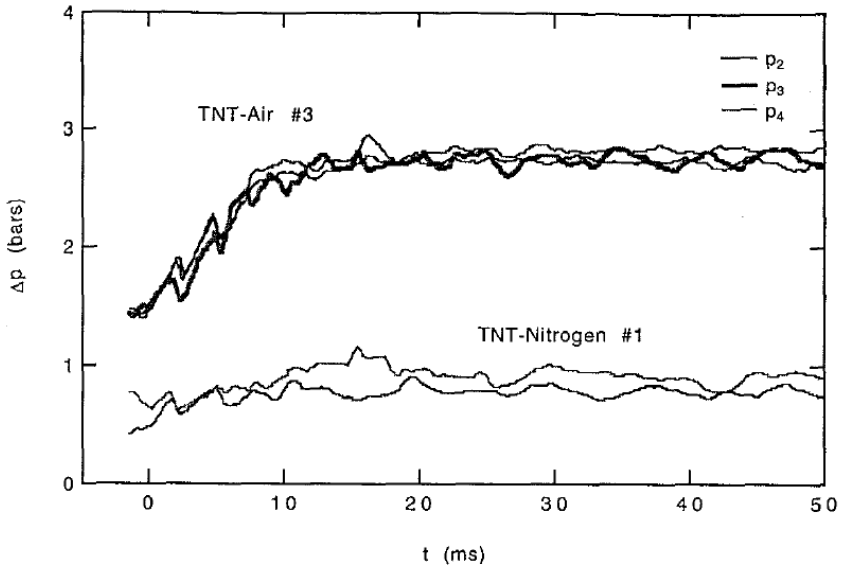

Figure 3 Reproduce Figure 7 from Kuhl et al. showing time averaged pressure histories for TNT detonated in air and nitrogen.

No Afterburning

There are several numerical parameters to be considered for the non-afterburn case before proceeding to the afterburn case:

- Mesh refinement – 2.5 versus 5mm
- Advection method –
  - Van Leer + Half-Index-Shift (HIS), second order accurate (METH=2) or
  - donor cell + HIS, first order accurate, conserving total energy over each advection step instead of conserving internal energy (METH=3)
- JWL EOS parameters –
  - Lee, Finger & Collins, January 1973 or
  - B.M. Dobratz, P.C. Crawford, January 31 1985
- Artificial bulk viscosity – AUTODYN versus LS-DYNA defaults

Mesh Refinement

Figure 4 compares the pressure and impulse histories at Tracer Particle 7, top of tank at half the radius refer back to Figure 1, for the two mesh refinements. The impulse at 60ms increases from 3.83 to 4.04MPa-ms for the more refined 2.5mm mesh spacing. It would be best in the case of making a prediction to perform another level of mesh refinement, but for the present purposes the 2.5mm mesh results will suffice and form the baseline for additional comparisons.

One way to estimate the residual chamber pressure is a moving average as was done in Kuhl et al.; that requires the complete digital gauge record to reproduce the 7.5ms move average results. However, a simpler approximation of the final chamber pressure is to assume the pressure is *constant over the duration* and divide the maximum impulse by the duration (impulse/duration). The justification for this estimation technique is noting the impulse is essentially increasing linearly, i.e. implying the pressure is constant. Also, integrating the pressure history for the nitrogen filled chamber, shown previously in Figure 2, and dividing by the 25ms duration produces an impulse/duration average pressure of 77kPa which is 9% less than the 85kPa measurement. The corresponding impulse/duration chamber pressures for the 5 and 2.5mm mesh are 64 and 67kPa, respectively. In terms of relative error with respect to the LLNL cited 85kPa residual pressure, these values under predict the measurement by 21 and 25%, respectively. An alternative approach for estimating the final pressure is to use a cumulative average of the pressure histories. The corresponding pressures for the 5 and 2.5mm mesh are 70 and 64kPa, respectively. Table 1 summarizes the no afterburn chamber residual pressures from the mesh refinement studies.

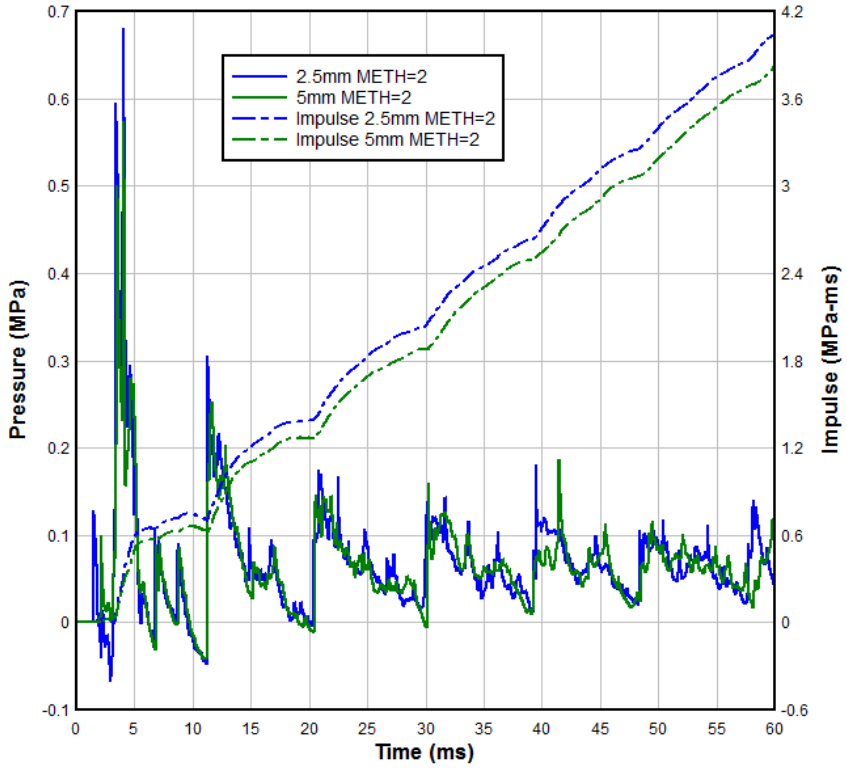

Figure 4 No afterburn pressure and impulse history comparison for 2.5 and 5mm uniform mesh discretization.

Table 1 Summary of no afterburn chamber residual pressures (kPa) for mesh refinement study.

LLNL	Impulse/Duration		Cumulative Average	
Reported	5mm	2.5mm	5mm	2.5mm
85kPa	64	67	70	64
% Diff	-25%	-21%	-18%	-25%

Advection Method

LS-DYNA offers four advection methods and typically METH=2, i.e. Van Leer + HIS (Half-Index-Shift) is recommended as it is second order accurate – in spatial discretization. An alternative advection method (METH=3) is recommend for models that explicitly include explosive materials – due to the large expansion ratio of the solid explosive into the detonation products. As with most multi-choice numerical parameters or methods, it is good practice to explore all appropriate options. Figure 5 compares the pressure and impulse histories at Tracer Particle 7 for the 2.5mm mesh refinement using the two advection choices.

The maximum impulses are 4.04 and 4.87MPa-ms for METH=2 and METH=3, respectively. The corresponding impulse/duration estimated residual pressures are 67 and 81kPa, respectively. These values under predict the LLNL measurement by 21 and 5%, respectively. The residual pressures using the cumulative average are 70.4 and 78.8kPa, respectively. Since the measured pressure is known, 85kPa, METH=3 will be used as the baseline for this simulation, i.e. model

calibration. Table 2 summarizes the no afterburn chamber residual pressures from the mesh refinement studies.

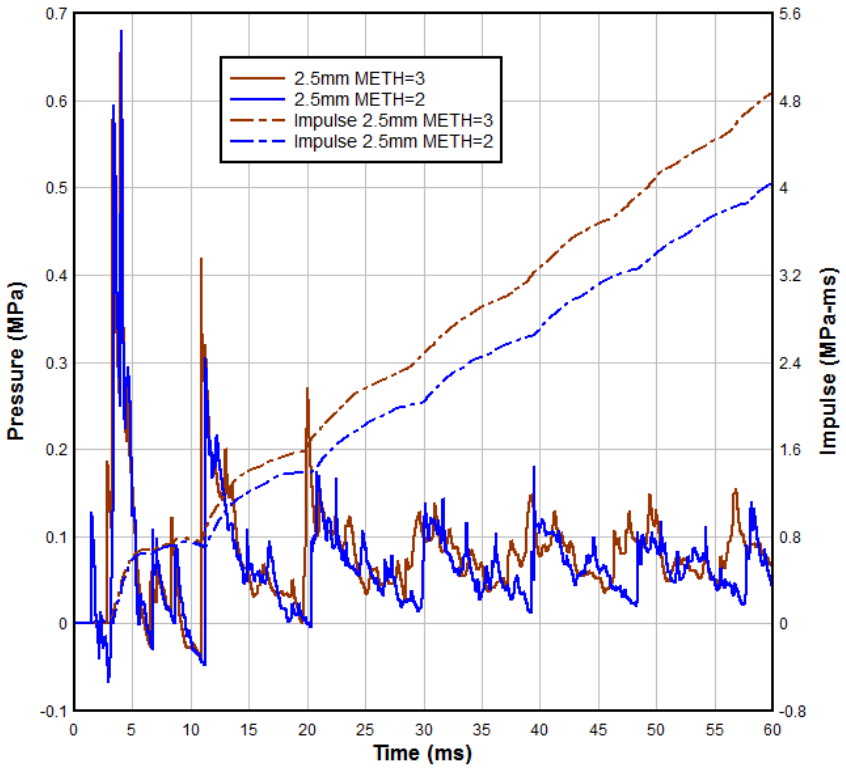

Figure 5 Pressure and impulse history comparison for 2.5mm mesh using two advection methods.

Table 2 Summary of no afterburn chamber residual pressures (kPa) for advection method study.

LLNL Reported	Impulse/Duration		Cumulative Average	
	METH=2	METH=3	METH=2	METH=3
85kPa	67	81	70	79
% Diff	-21%	-5%	-18%	-7%

JWL EOS Parameters

AUTODYN, used by Edri et al. (2013), offers two sets of TNT JWL parameters denoted as TNT (Lee, Finger & Collins, 1973) and TNT-2[2] (Dobratz & Crawford, 1985). There are several differences in the JWL parameters, but the two most notable are the C-J energy per unit volume $E_0 = 6\times10^6$ kJ/m^3 for TNT and $E_0 = 7\times10^6$ kJ/m^3 for TNT-2 and the EOS parameter $\omega = 0.35$ for TNT and $\omega = 0.30$ for TNT-2; see Table 3[3]. Figure 6 compares the pressure and impulse

[2] AUTODYN provides default JWL EOS parameters and uses the terminology TNT and TNT-2 to distinguish between them.

[3] Two additional sets of JWL parameters is provided by Poon et al. (2014) and listed in an appendix for the reader's convenience.

histories at tracer particle 7 for the 2.5mm mesh refinement, using METH=3 and the two sets of JWL parameters.

Table 3 Comparison of AUTODYN JWL parameters for TNT.

JWL Parameter	TNT	TNT-2
A (GPa)	373.75	371.25
B (GPa)	3.747	3.231
R_1	4.15	4.15
R_2	0.90	0.95
ω	0.35	0.30
E_0 (GPa)	6.0	7.0

The maximum impulses are 4.87 and 5.51MPa-ms for the TNT and TNT-2 parameters, respectively. The corresponding impulse/duration estimated residual pressures are 81 and 92kPa, respectively. The AUTODYN-TNT parameters under predict the LLNL measurement of 85kPa by 5% and the TNT-2 parameters over predict the measurement by 8%. The residual pressures using the cumulative average are 78.8 and 89.1kPa, respectively. The TNT-2 JWL parameters will be used in the baseline since Dobratz & Crawford in 1985 were aware of the parameters proposed by Lee, Finger & Collins in 1973, i.e. see Reference 58 in Dobratz & Crawford, and chose to change them. Table 4 summarizes the no afterburn chamber residual pressures from the TNT parameter studies.

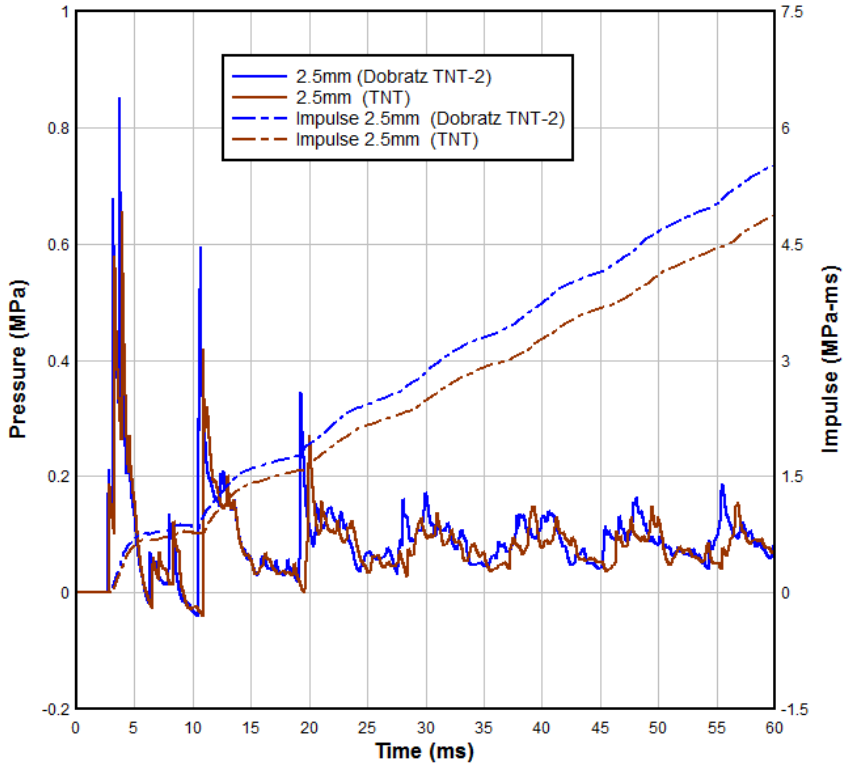

Figure 6 Pressure and impulse history comparison for 2.5mm mesh, METH=3 and two sets of JWL EOS parameters.

Table 4 Summary of no afterburn chamber residual pressures (kPa) for TNT parameter study.

LLNL Reported	Impulse/Duration		Cumulative Average	
	TNT	TNT-2	TNT	TNT-2
85kPa	81	92	79	89
% Diff	-5%	8%	-7%	5%

Artificial Bulk Viscosity

The default quadratic and linear artificial bulk viscosity parameters used by AUTODYN are $Q_1 = 1.0$ and $Q_2 = 0.2$ and the corresponding LS-DYNA default parameters are $Q_1 = 1.5$ and $Q_2 = 0.06$. Using the 2.5mm mesh with METH=3 and the Dobratz & Crawford (TNT-2) JWL EOS parameters, there was no difference in the results for these two sets of artificial bulk viscosity parameters.

Comparison with Edri's AUTODYN Results

Figure 7 compares the pressure and impulse histories at Tracer Particle 7 from the Edri's AUTODYN 5mm mesh using AUTODYN-TNT JWL parameters[4] with the LS-DYNA 2.5mm, METH=3 and TNT-2 JWL parameters. The default advection algorithm used by AUTODYN is not presently known to the author.

The maximum impulses are 6.58 and 5.51MPa-ms for the AUTODYN and LS-DYNA baseline parameters, respectively. The corresponding impulse/duration estimated residual pressures are 110 and 92kPa, respectively. The AUTODYN simulation over predicts the LLNL measurement by 29% and the LS-DYNA baseline over predicts the measurement by 8%. The residual pressures using the cumulative average are 106.2 and 89.1kPa, respectively. Table 5 summarizes the no afterburn chamber residual pressures from AUTODYN and LS-DYNA.

[4] Figure 5 in Edri et al (2013). The digital pressure history was kindly provided by Idan Edri.

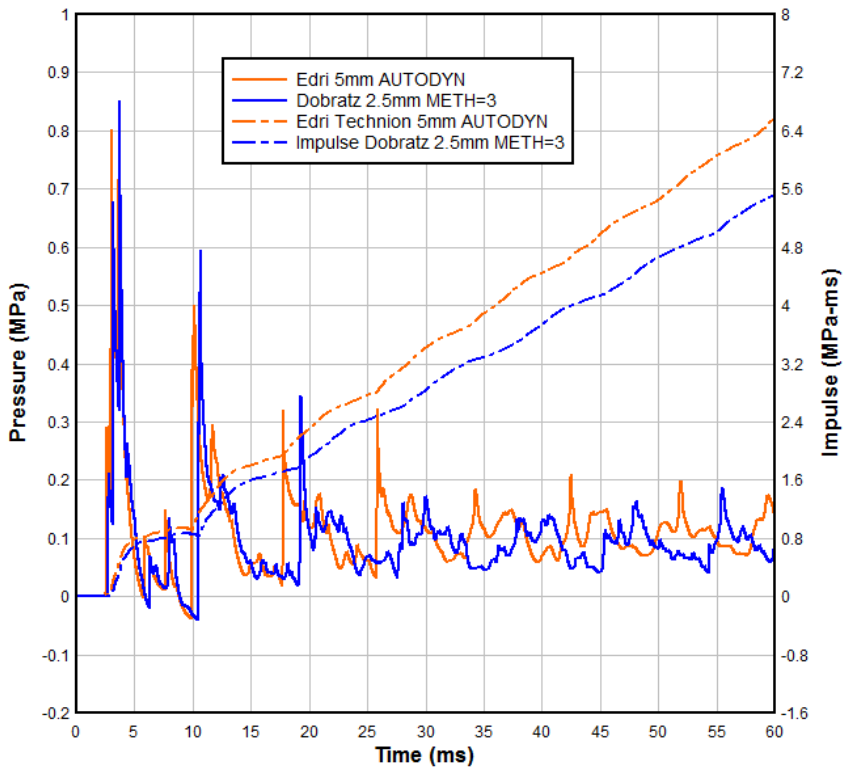

Figure 7 Pressure and impulse history comparison for Edri's 5mm AUTODYN mesh with the LS-DYNA baseline parameters.

Table 5 Summary of no afterburn chamber residual pressures (kPa) for AUTODYN and LS-DYNA.

LLNL Reported	Impulse/Duration		Cumulative Average	
	AUTODYN	LS-DYNA	AUTODYN	LS-DYNA
85kPa	110	92	106	89
% Diff	29%	8%	25%	5%

Non-Afterburning Results Summary

In what should be a fairly straightforward numerical simulation of a TNT charge in an enclosed chamber without afterburning, it is demonstrated that *basic modeling options*, i.e. mesh refinement, advection method and JWL parameter selection, produce LS-DYNA results that under predict the measurement by as much as 25% and over predict by 8%.

The reader should anticipate there will be even more variation in the simulation results for the more complex afterburning results.

Afterburning

In this section the LLNL reported chamber residual pressure for the TNT detonated in air are compared with two results from Edri et al. (2013) and the LS-DYNA afterburn model results.

Edri's Simulations

Edri et al. (2013) presented two calculations of the LLNL afterburning experiment:

1. MM-ALE simulation using the simple afterburning algorithm available in AUTODYN,
2. A clever empirical pressure shift of the non-afterburn pressure history to account for the afterburning energy.

These are discussed in the appendices.

Edri's Results

Figure 8 compares the pressure and impulse histories from the LLNL-HEAF test in air with Edri et al. (2013) results using AUTODYN's simple afterburn model, and shifting the no afterburn pressure history. The inputs for the AUODYN simple afterburn model are additional afterburn energy of 10 MJ/kg starting at 2.4 and ending at 4.4ms. For the shifting of the no afterburn pressure history, the no afterburn pressure history was shifted using $K_{ab} = 3.0$ for times greater than 9.92ms using the afterburning residual pressure value of 0.106MPa. The late time corresponds to the second pressure peak in the no afterburning pressure history and the residual pressure was obtained from the cumulative average.

The maximum impulses are 13.39MPa-ms at 51.8ms for the LLNL data, 15.28 and 17.14MPa-ms at 60ms for the AUTODYN simple afterburn simulation and shifted no afterburn results, respectively. The corresponding estimated residual pressures from the impulse/duration are 259kPa for the LLNL data [280KPa was reported by Kuhl et al. (1998)] and 255 and 286kPa for the AUTODYN simple afterburn simulation and shifted no afterburn results, respectively. The residual pressures using the cumulative average are 266kPa for the LLNL data, and 253 and 252kPa for the AUTODYN simple afterburn simulation and shifted no afterburn results, respectively. The AUTODYN simple afterburn model and the shifted no afterburn results, using the cumulative average residual pressure, both under predicted the reported LLNL residual pressure of 280kPa by 10%. Table 6 summarizes the afterburn chamber residual pressures from Edri's afterburn and shifted pressure results.

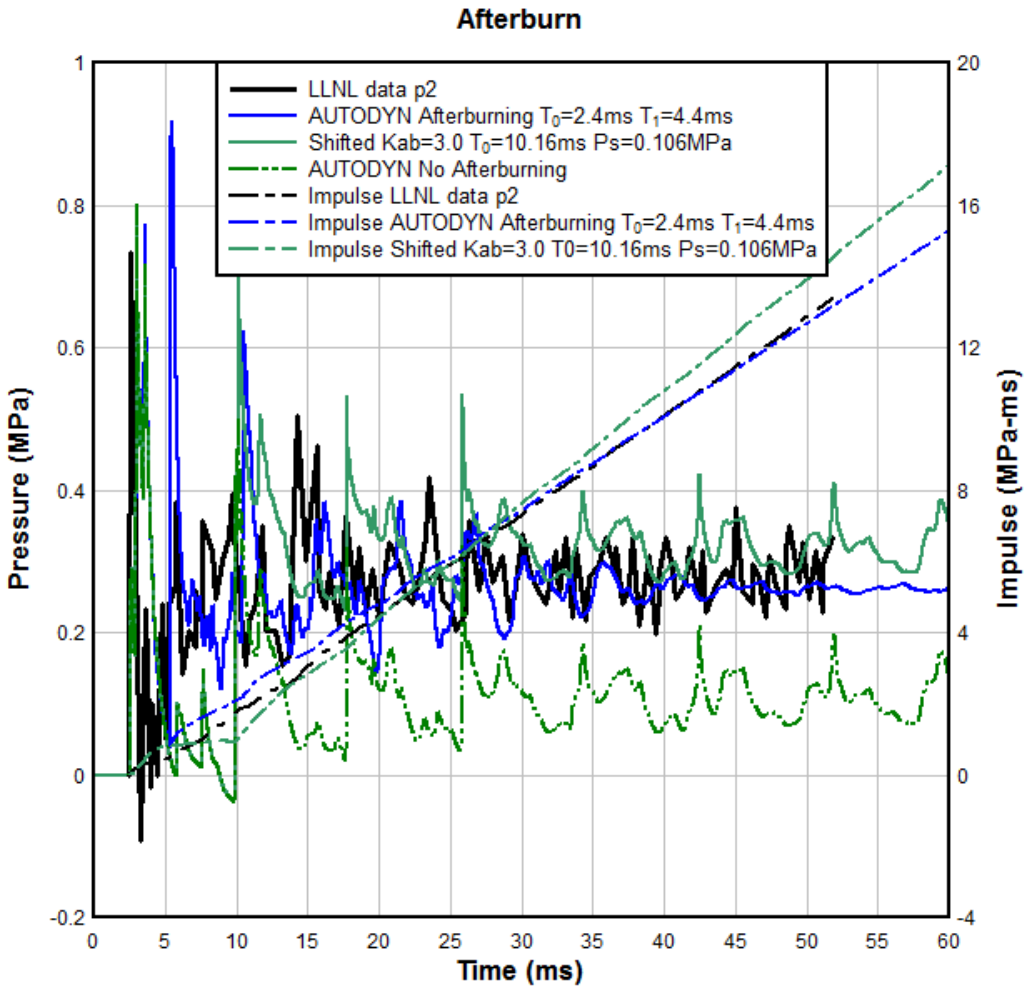

Figure 8 Pressure and impulse history comparison of LLNL HEAF afterburning data with Edri's AUTODYN afterburning model, and shifted no afterburning approximation.

Table 6 Summary of afterburn chamber residual pressures (kPa) from Edri's afterburn and pressure shifted results.

LLNL Reported	Impulse/Duration			Cumulative Average		
	LLNL	Afterburn	Shifted	LLNL	Afterburn	Shifted
280kPa	239	255	286	266	253	252
% Diff	-15%	-9%	2%	-5%	-10%	-10%

LS-DYNA Simulation

The newly implemented afterburn model in LS-DYNA offers two major options:

1. A simple afterburning algorithm modeled after the AUTODYN's implementation, with an optional constant or linearly increasing rate of the additional afterburning energy,
2. The so called "Miller's Extension", Miller, (1996), model of afterburning.

Briefly, Miller's Extension for afterburn energy adds the energy Q to the JWL equation-of state via a time dependent growth term:

$$Q = \lambda Q_0$$
$$\frac{d\lambda}{dt} = a\left(1-\lambda\right)^m P^n$$

where the parameters a, m and n, in addition to Q_0, are required user inputs; Miller (1996) cites values of $m = 1/2$ and $n = 1/6$ in demonstrating his model.

LS-DYNA Afterburning Results

The simple afterburning LS-DYNA model input parameters are $Q_0 = 16.3\text{GPa} = \left(10\text{MJ/kg}\right)\left(1630\text{kg/m}^3\right)$ starting at 2.4 and ending at 4.4ms with a linearly increasing addition of the afterburning energy. The pressure and impulse histories for the LLNL data and the AUTODYN and LS-DYNA simple afterburn models are shown in Figure 9. The maximum impulses are 13.39MPa-ms at 51.8ms for the LLNL data, 15.28MPa-ms at 60ms for the AUTODYN simple afterburn model and 14.59MPa-ms at 60ms[5] for the LS-DYNA simple afterburn model. The corresponding estimated residual pressures from the impulse/duration are 259kPa for the LLNL data (280Kpa was reported by Kuhl et al.), 255kPa for the AUTODYN simple afterburn model and 223kPa for the LS-DYNA simple afterburn model. Table 7 summarizes the afterburn chamber residual pressures from Edri's AUTODYN and the LS-DYNA afterburn simulations.

[5] Note: the LS-DYNA after burn model requires a significant amount of amount of CPU time, i.e. almost 163 hours on a single 2.4GHz processor Windows laptop; the non after burn case required about 4 CPU hours using four CPUs, i.e. about 16 CPU hours total. Edri et al. also mentions a significant, factor of 9, increase in CPU for the simple after burning model over the non-after burning simulation.

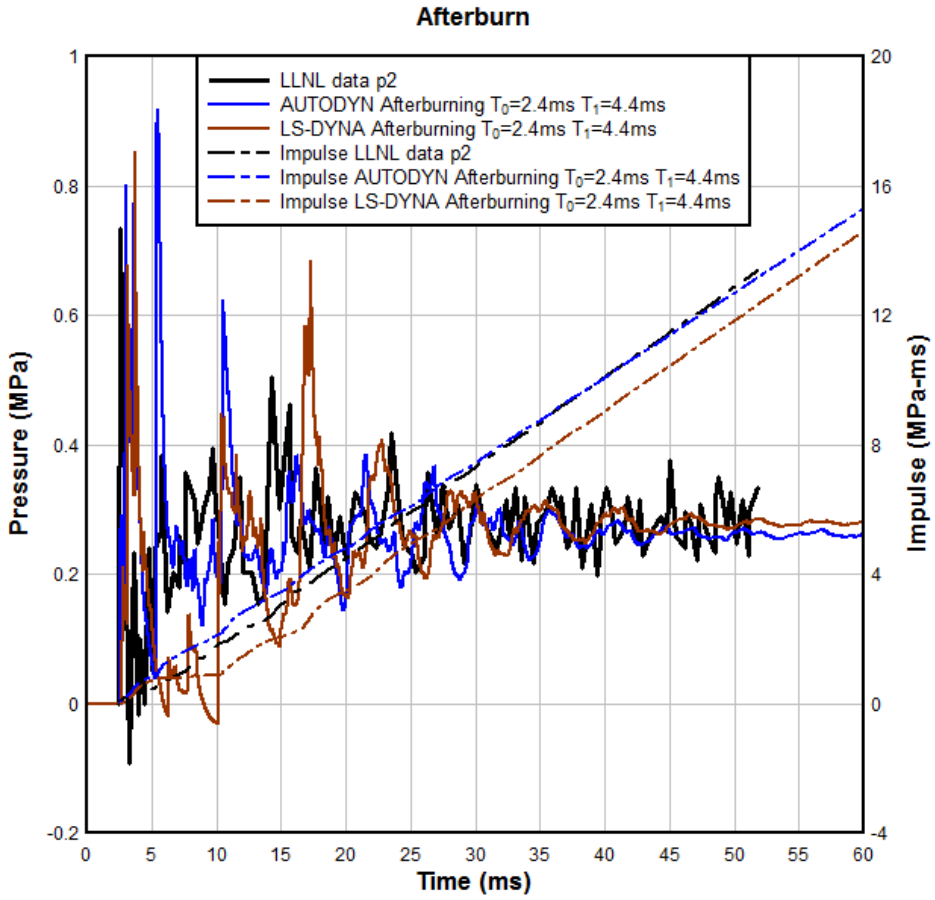

Figure 9 Pressure and impulse history comparisons of LLNL HEAF afterburning data with Edri's AUTODYN afterburn model and the corresponding LS-DYNA afterburn model.

Table 7 Summary of afterburn chamber residual pressures (kPa) from Edri's AUTODYN and the LS-DYNA afterburn simulations.

LLNL Reported	Impulse/Duration	
	AUTODYN	LS-DYNA
280kPa	255	223
% Diff	-9%	-20%

Figure 10 shows a comparison of the pressure histories, and cumulative averages, for the two simple afterburn models, i.e. AUTODYN and LS-DYNA. The major difference in these pressure histories occurs after about 5ms, i.e. coincidently (?) the end of the afterburning energy. Between about 5 and 10ms, the LS-DYNA pressure drops to near zero while the AUTODYN pressure is nearly constant at about 0.2MPa. It is this early time drop in the LS-DYNA pressure that causes both its residual pressure, derived from cumulative average and impulse/duration, to be less than the AUTODYN residual pressure. However, at 60ms the LS-DYNA pressure is 0.28MPa which slightly greater than the 0.26MPa provided by AUTODYN at 60ms, and agrees with the 0.28MPa pressure reported by Kuhl et al.

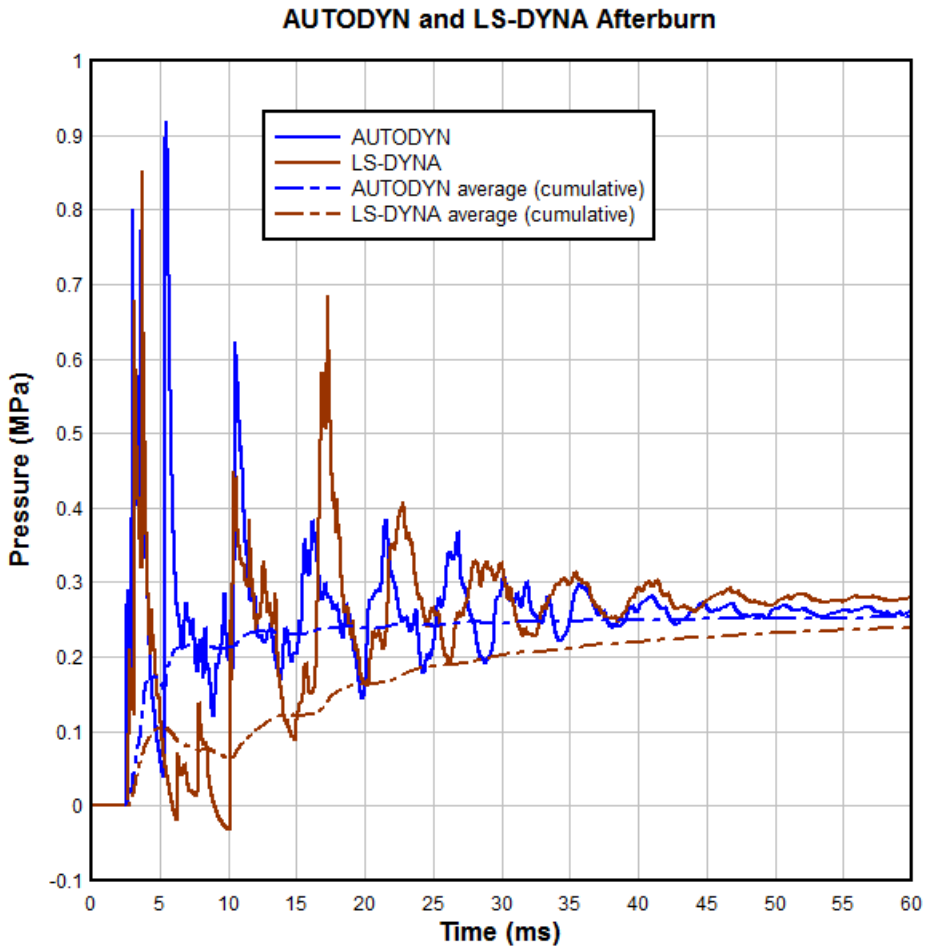

Figure 10 Comparison of AUTODYN and LS-DYNA pressure histories for simple afterburning models.

Simulation of NCEL Tests

Keenan and Wager, (1992) discuss results from tests conducted in 1991 by the Carderock Division of the Naval Surface Warfare Center (NSWC), Code 1740.2, on high explosives for the Naval Civil Engineering Laboratory (NCEL). These tests were in support of NCEL development of the High Performance (HP) Magazine. As part of this test series to assess the effectiveness of water barriers in magazines designed to safely contain explosives, a baseline test without the water, i.e. a bare explosive charge, was conducted. It is this bare change in a confined cylindrical environment that is of present interest. Subsequently, Birnbaum et al. (1998) and Edri et al. (2013) used AUTODYN to simulate the tests and reported the pressure history.

The present work seeks to calculate the NCEL bare charge test using the newly implemented LS-DYNA afterburning JWL equation-of-state. First the non-afterburning data is used to examine two of the ancillary computational parameters associated with detonation and air blast simulations, i.e. mesh refinement and JWL parameters.

NCEL Tests

The tests were conducted by the Carderock Division of the Naval Surface Warfare Center in a closed cylindrical chamber. The following charge and chamber descriptions are from Keenan and Wager (1992):

> "In all tests, the weight of explosive, W, was 4.6 lb TNT, the test chamber volume, V, was l,150 ft^3, and the vent area of the chamber, A , was 0 ft^2."

Both Birnbaum et al. and Edri et al. (2013) modeled the NCEL test configuration as axisymmetric with half the length of the chamber. The chamber radius was 1.73m as was the half height of the chamber. This provides for a total chamber volume of 32.53 m^3 (1150ft^3). The 2.12kg (4.6lbf) TNT charge is also modeled as a cylinder with length-to-diameter ratio of one and a 59.15mm radius and half length.

Keenan and Wager do not provide information on the number or location of the pressure diagnostics. However, since the quantity of interest is the final pressure in the tank, the location of the gauges in not required, as all gauges should have the same final pressure.

NCEL Test Model

A Multi-Material ALE (MM-ALE) axisymmetric model of the half-length cylinder was created using uniform 5 and 2.5mm meshes, see Figure 11. All four exterior edges of the mesh were constrained from normal displacement. The simulated tank was filled with air modeled as an ideal gas. The TNT charge was included in the model using the LS-DYNA keyword *INITIAL_VOLUME_FRACTION_GEOMETRY to fill the corresponding MM-ALE region. For the 5mm mesh spacing there are almost 12 cells across the radius of the charge, which is close to the rule-of-thumb minimum 10 cells; the 2.5mm mesh discretization, with 23 cells across the charge radius, results are compared with the 5mm mesh results as one of the modeling parameters. The 2.12kg TNT charge was center detonated and modeled using the JWL equation-of-state with parameters obtained from Dobratz & Crawford (1985) and the AUTODYN default TNT EOS due to, Lee, Finger & Collins (1973). The indicated eight tracer particle locations are those shown in Birnbaum et al. (1998) and adopted by Edri et al. (2013).

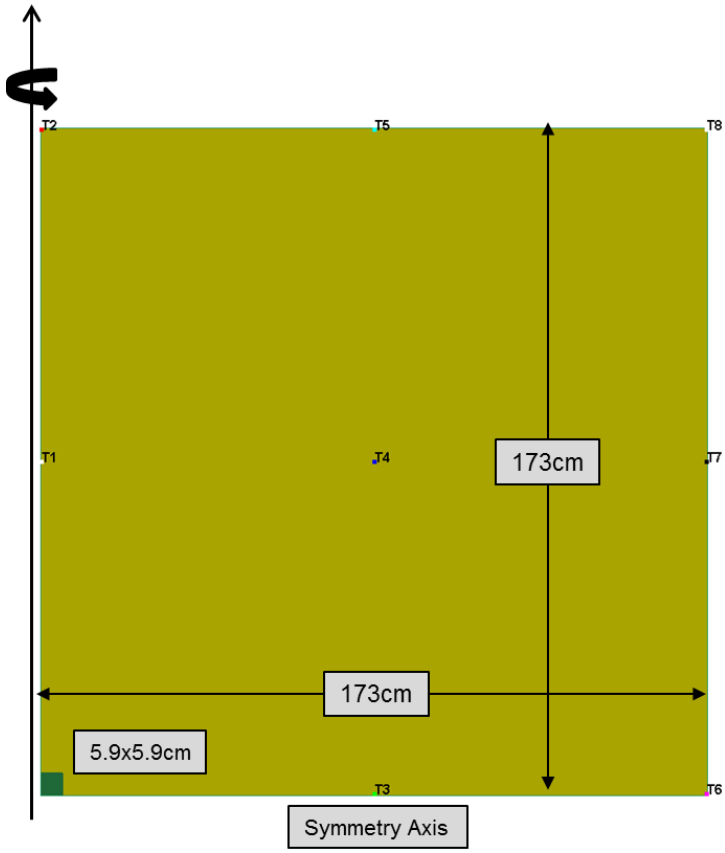

Figure 11 Axisymmetric half-length model of the NCEL cylinder with locations of 8 tracer particles indicated.

Simulation Results

Before attempting the afterburning simulation, the above described model was used to simulate the non-afterburning case. Unfortunately, no non-afterburning test was reported by NCEL so the only data available, without water in the closed chamber, is shown here as Figure 12. For this case the reported residual pressure was 51.3psi (3.54bar).

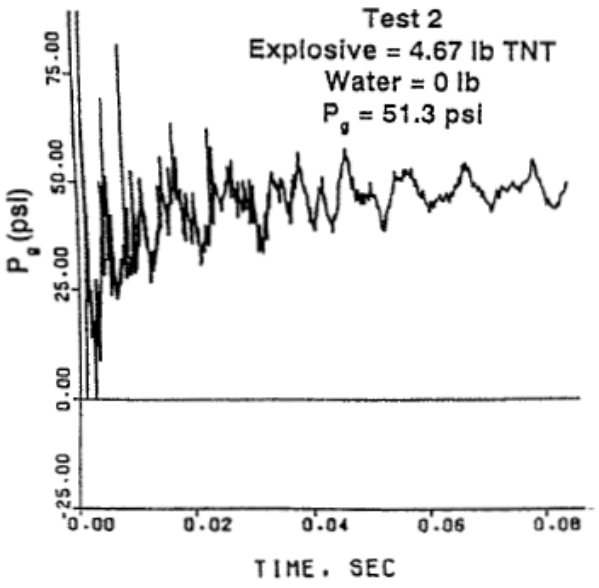

Figure 12 Pressure history without water in closed cylindrical chamber as reported in Keenan and Wager (1992) as their Figure 2b.

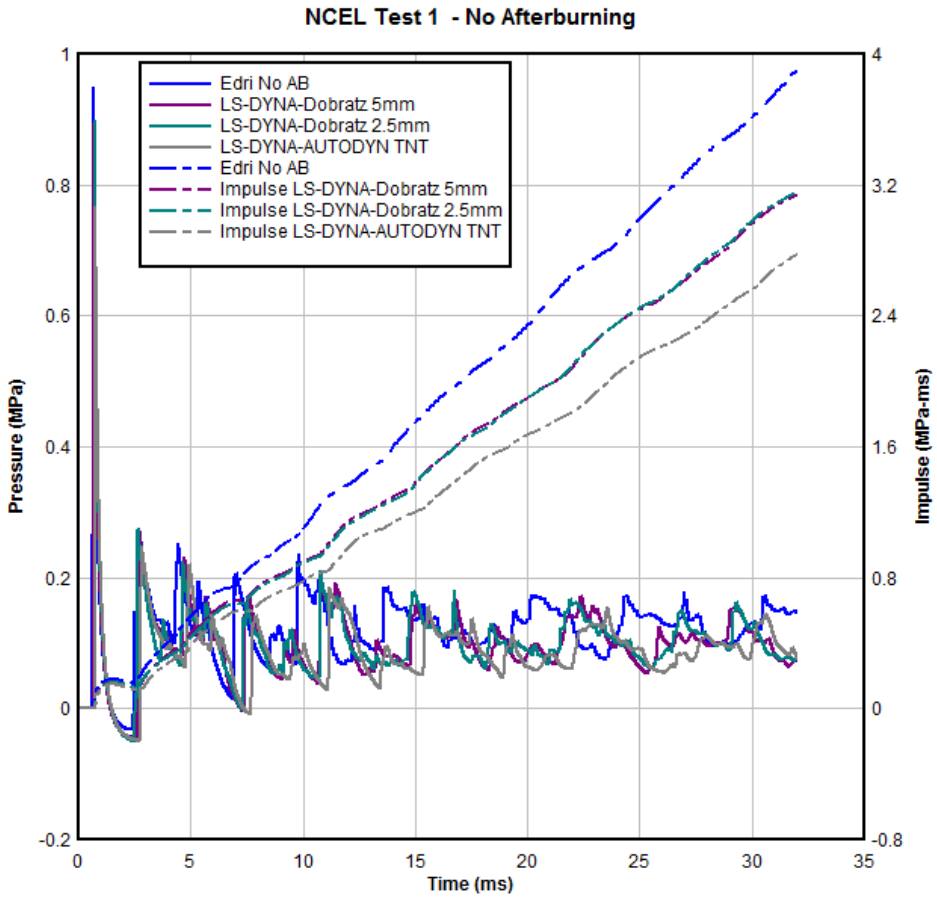

Figure 13 Comparison of Edri no afterburning NCEL simulation and three LS-DYNA no afterburning parameter study results.

No Afterburning

Figure 13 shows the no afterburning pressure and impulse results from Edri et al. (their Figure 7) of the NCEL test along with corresponding LS-DYNA results. LS-DYNA parameter variation results were:

- The impulse results for the 2.5 and 5mm mesh sizes, using the Dobratz TNT EOS, are nearly identical, i.e. 3.15MPa-ms,
- The lowest impulse value, 2.77MPa-ms, corresponds to the 5mm mesh using the AUTODYN default TNT parameters.

For all three LS-DYNA calculations, the total energy conserving METH=3 advection method was used.

To estimate the final chamber pressures for the no afterburning case, the maximum impulses are divided by the corresponding duration:

- Edri et al 0.122MPa (=3.9MPa-ms/32ms)
- LS-DYNA 2.5 and 5mm mesh with Dobratz TNT 0.098MPa (=3.15MPa-ms/32ms)
- LS-DYNA 5mm mesh with AUTODYN TNT 0.087MPa (=2.77MPa-ms/32ms)

If a cumulative average is used to estimate the residual pressures, the results are similar:

- Edri et al 0.116MPa
- LS-DYNA 2.5 and 5mm mesh with Dobratz TNT 0.092MPa
- LS-DYNA 5mm mesh with AUTODYN TNT 0.080MPa

Also, Birnbaum et al. provided an AUTODYN result for the no afterburn case with an estimated residual pressure of 0.13MPa that closely agrees with Edri's result. The LS-DYNA Dobratz JWL parameters residual pressure underestimates Birnbaum's result by about 25%. Recall there is no experimental result for the non-afterburn case. Table 8 summarizes the non-afterburn chamber residual pressures from Birnbaum and Edri's AUTODYN results and the LS-DYNA non-afterburn simulations.

Table 8 Summary of the non-afterburn chamber residual pressures (MPa) from Birnbaum and Edri's AUTODYN results and the LS-DYNA non-afterburn simulations.

Birnbaum	Impulse/Duration			Cumulative Average		
Reported	AUTODYN	Dobratz	Lee	AUTODYN	Dobratz	Lee
0.13MPa	0.122	0.098	0.087	0.116	0.092	0.08
% Diff	-6%	-25%	-33%	-11%	-29%	-38%

Afterburning

Edri et al. (2013) provide afterburning results for the NCEL test using the AUTODYN simple afterburning model and their non-afterburning pressure history shifting method. The LS-DYNA afterburning results also use a simple afterburning model, similar to the AUTODYN model. These afterburning models are briefly described in the appendix.

Edri et al. Results

Figure 14 compares the pressure and impulse histories from Edri et al. (2013) using AUTODYN's simple afterburn model, and their shifting of the no afterburn pressure history. The inputs for the AUTODYN simple afterburn model are additional afterburn energy of 10 MJ/kg starting at 1.4 and ending at 4.4ms. For the shifting of the no afterburn pressure history, the no afterburn pressure history was shifted using $K_{\text{ab}} = 3.0$ for times greater than 2.75ms using the residual pressure value of 0.116MPa. This time corresponds to the second pressure peak in the no afterburning pressure history and the residual pressure obtained from its cumulative average.

The start time, 1.4ms, for the simple afterburning model is estimated as corresponding to the end of the first pressure pulse, i.e. the pressure at the tracer particle (#4) returns to zero due to reflected shock from distant boundary allowing shock mixing of the air with the detonation products for additional afterburning. The end of the additional afterburning, 4.4ms, corresponds to the time at which the temperature in the gas drops below that needed to sustain burning in the detonation products, i.e. about 900K. AUTODYN outputs the temperature at tracer particles, but it is not known how this temperature is calculated. For an idea gas the relation between temperature and internal energy is given by:

$$T = E / C_v$$

here C_v is the heat capacity at constant volume and is not known for the mixture of air and detonation products. However, if we assume $C_v = 0.834$ kJ/(kg-K)[6] at 900K, then at an internal energy less than about 750 kJ/kg the afterburning would terminate.

For the shifting of the no afterburn results, it is difficult to justify an energy ratio term K_{ab} less than 3.0 for the small charge mass to volume ratio of 0.065 kg/m^3 (8.39×10^{-4} lbf/ft^3), see Edri et al. (2013) Figure 4. Limited experience with shifting the no afterburn pressure history to *estimate* the afterburning pressure history, i.e. only two cases with small charge mass to volumes ratios, has not provided sufficient experience to provide additional guidance about selecting values of K_{ab}.

[6] https://www.ohio.edu/mechanical/thermo/property_tables/air/air_Cp_Cv.html (URL last checked 25Jul15)

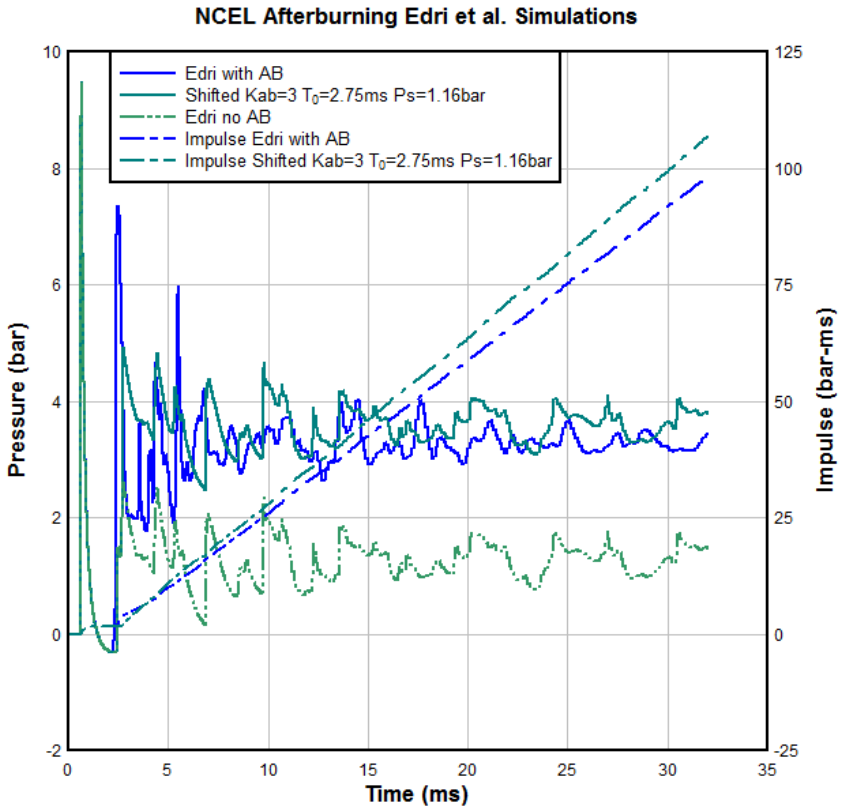

Figure 14 Pressure and impulse history comparison of Edri's AUTODYN afterburning model and shifted no afterburning approximation.

Figure 15 compares the pressure and impulse histories from the NCEL test[7] with the previously shown Edri et al. (2013) results using AUTODYN's simple afterburn model, and shifting the no afterburn pressure history. The maximum impulses and corresponding estimated residual pressures from the impulse/duration and cumulative average are:

- NCEL Test – 2.94 bar (94.50 @ 32ms) – cumulative average 2.88bar
- Edri Afterburn – 3.07bar (98.22 @ 32ms) – cumulative average 2.99bar
- Edri Shifted – 3.34bar (106.94@ 32ms) – cumulative average 2.79
- Birnbaum et al. – 3.3bar

Table 9 summarizes the afterburn chamber residual pressures from Birnbaum and Edri's AUTODYN results.

The NCEL report, Keenan and Wager (1992), reported 3.54bar (51.3psi) as the residual chamber pressure. This pressure does not agree with either the pressure determined from impulse/duration or cumulative average. Referring back to Figure 12, i.e. the NCEL pressure history of Keenan and Wager (their Figure 2b), an 'eyeball' estimate of the residual pressure appears to be less than 50psi (3.54bar).

[7] The digital version of the NCEL pressure history was kindly provided by Idan Edri of the Technion.

Using the reported NCEL 3.54bar pressure, Edri's simulations both under predict the reported NCEL residual pressure by about 6 (shifted) and 13% (simple afterburn).

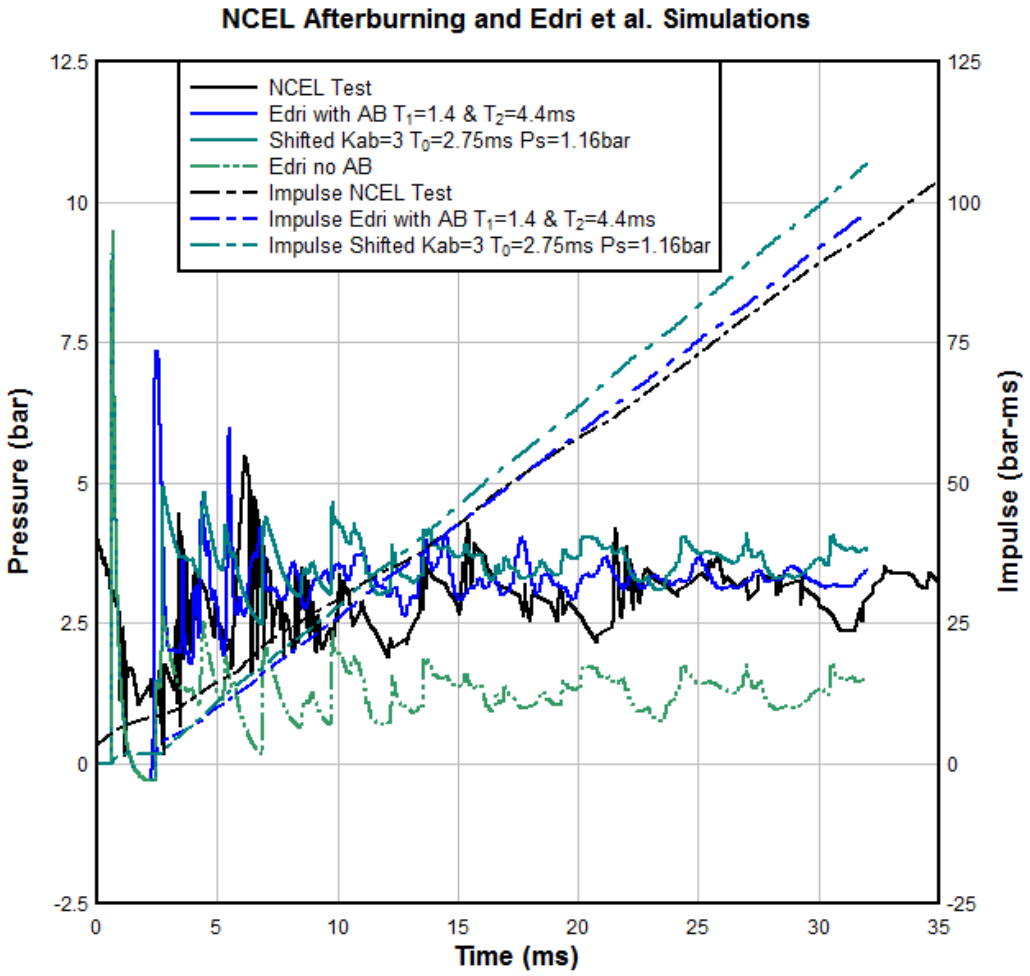

Figure 15 Pressure and impulse history comparison of NCEL afterburning data with Edri's AUTODYN afterburning model and shifted no afterburning approximation.

Table 9 Summary of the afterburn chamber residual pressures (bar) from Birnbaum and Edri's AUTODYN results.

	Impulse/Duration			Cumulative Average		
Birnbaum	NCEL	Afterburn	Shifted	NCEL	Afterburn	Shifted
3.3	2.95bar	3.07	3.34	2.88bar	2.99	2.79
12%	% Diff	4%	13%	% Diff	4%	-3%

LS-DYNA Simulation

The simple afterburning LS-DYNA model input parameters are $Q_0 = 16.3\text{GPa} = (10\text{MJ/kg})(1630\text{kg/m}^3)$ starting at 2.4 and ending at 4.4ms with a linearly increasing addition of the afterburning energy. The pressure and impulse histories for the NCEL data and the AUTODYN and LS-DYNA simple afterburn models are shown in Figure 16; the simulated pressure histories are from the center of the quarter model, i.e. Tracer Particle T4 refer back to Figure 11. The LS-DYNA maximum impulses and corresponding estimated residual pressures from the impulses and cumulative average are:

- LS-DYNA – 3.18bar (101.84 @ 32ms) – cumulative average 3.37bar.

The LS-DYNA residual pressure under predicts the NCEL pressure (3.54bar) by 10%, similar to Edri's simple afterburn model result.

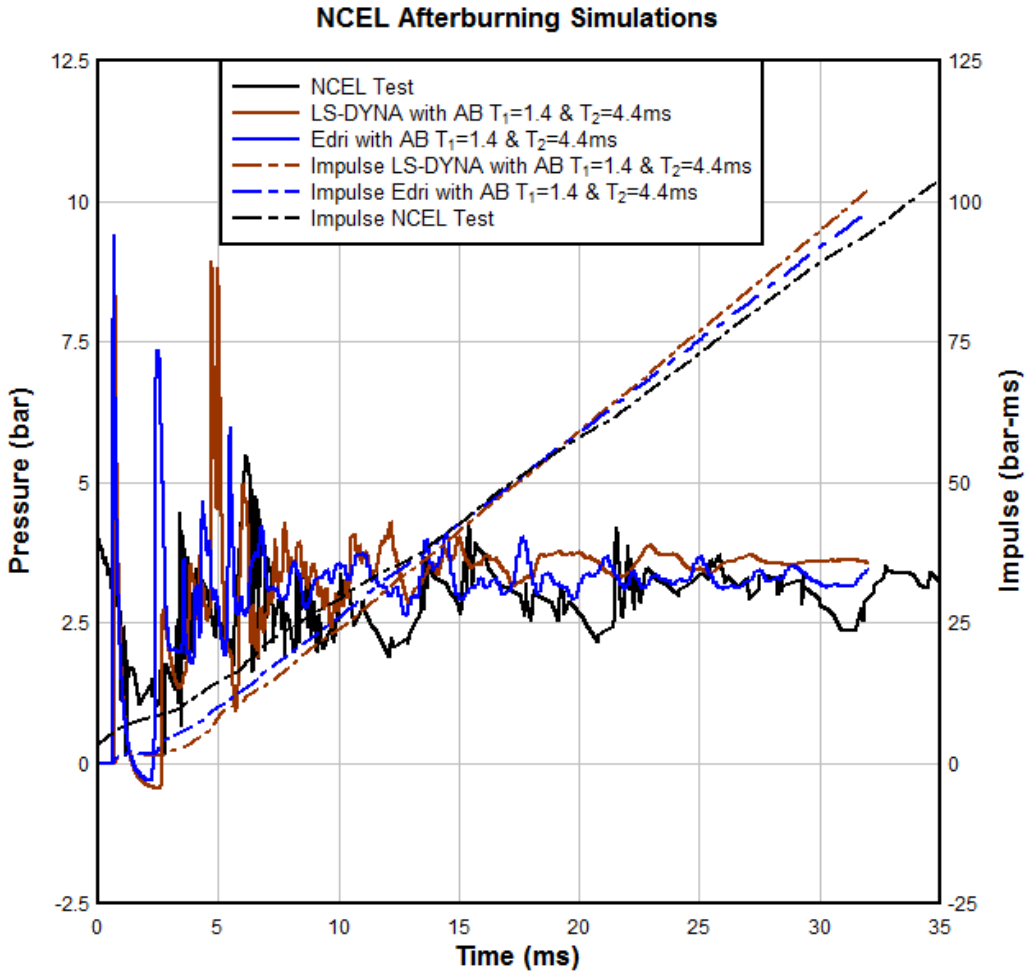

Figure 16 Pressure and impulse history comparisons of NCEL afterburning data with Edri's AUTODYN afterburn model and the corresponding LS-DYNA afterburn model.

Figure 17 is a bar chart displaying the residual pressure as reported by NCEL and Birnbaum, and Edri and LS-DYNA simulations, as derived from impulse/duration and cumulative average. Including both methods of determining the residual pressure provides a consistency check and an indication of the amount of variability in the values, especially when the method for obtaining the reported (experimental) values was not explicitly stated.

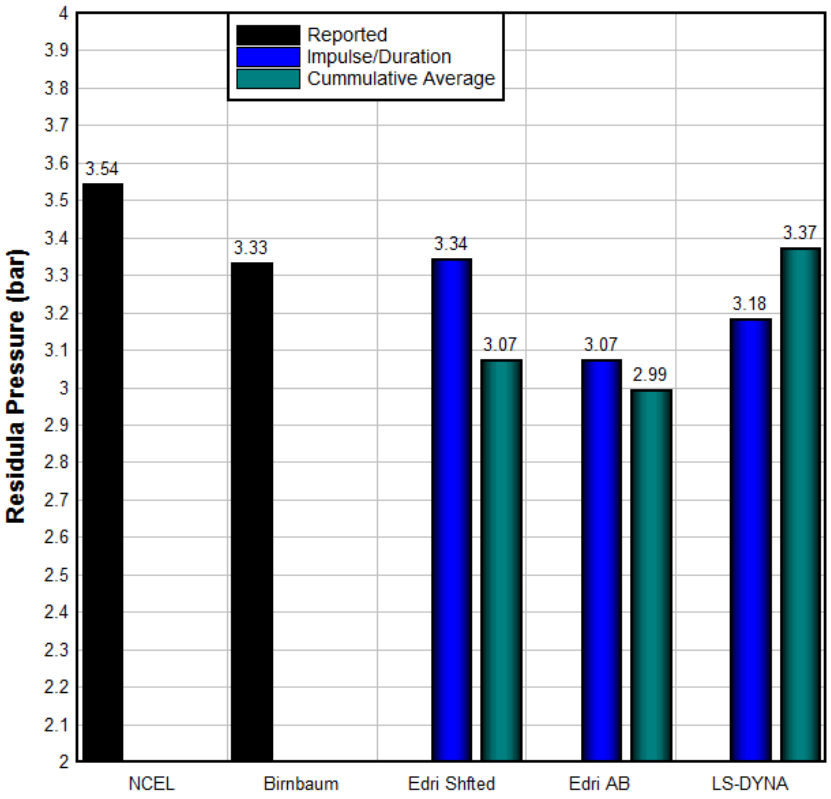

Figure 17 Residual pressure reported by NCEL and Birnbaum, and Edri and LS-DYNA simulation results derived from impulse/duration and cumulative average.

Finally, Figure 18 compares the pressure and cumulative average impulse histories for the AUTODYN and LS-DYNA simple afterburning models. For the NCEL simulation the two pressure histories agree fairly well until about 5ms, coincidently (?) the end of the additional afterburning energy (4.4ms), when some large pressure spikes are predicted in the LS-DYNA model. These pressure spikes cause the LS-DYNA cumulative average to exceed that of the AUTODYN simulation after 5ms. Also, note that the final values of the cumulative average do not reflect what might be 'eyeballed' as the residual pressures from the pressure histories.

A note on the CPU time comparison for the non-afterburning and afterburning cases: non-afterburning required about 4 CPU hours using 4 processors, about 16 CPU hours, while the afterburning case required 122 hours using a single CPU. The present developmental afterburning model has not yet been incorporated in the multiple CPU version of LS-DYNA.

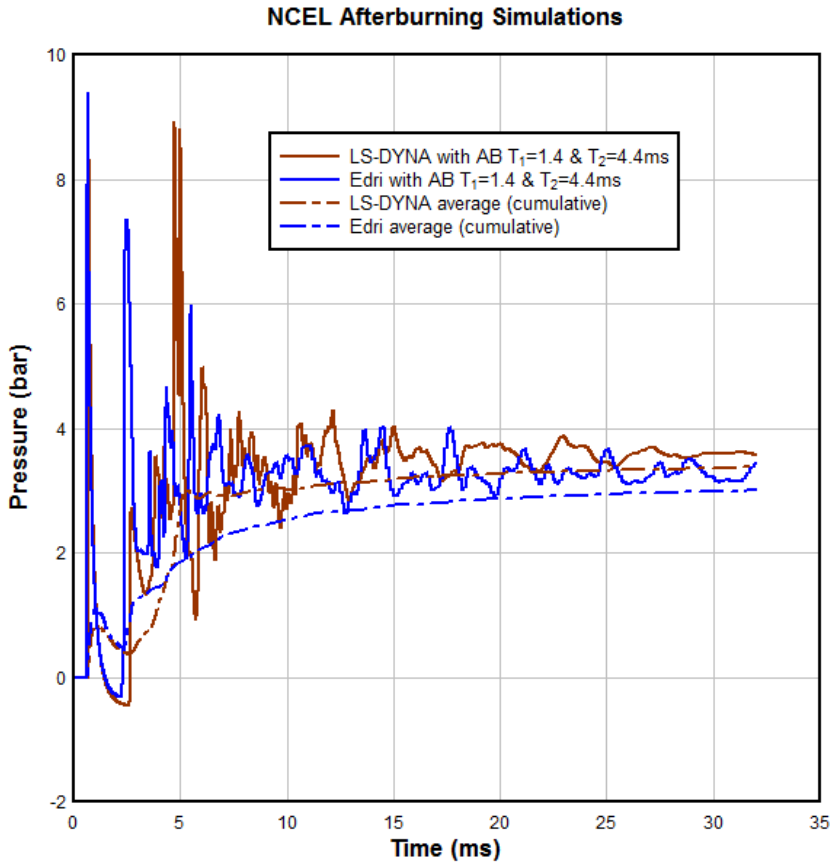

Figure 18 Comparison of AUTODYN and LS-DYNA pressure histories, and cumulative averages, for simple afterburning models.

Simulation of Moby Dick Explosive Tests

Miller & Guirguis (1993) conducted small scale laboratory tests to calibrate their time dependent variation of the Jones-Wilkens-Lee (JWL) equation of state, often referred to as the Miller Extension. A schematic of the laboratory test apparatus is shown in Figure 19. It consists of a cube of steel, 80cm on a side, with a 2.5cm hole in the top that admits a Lexan tube of the same outer diameter with an inner diameter of 6.25mm. The 1m length of Lexan tube is filled with water that sits atop the explosive charge.

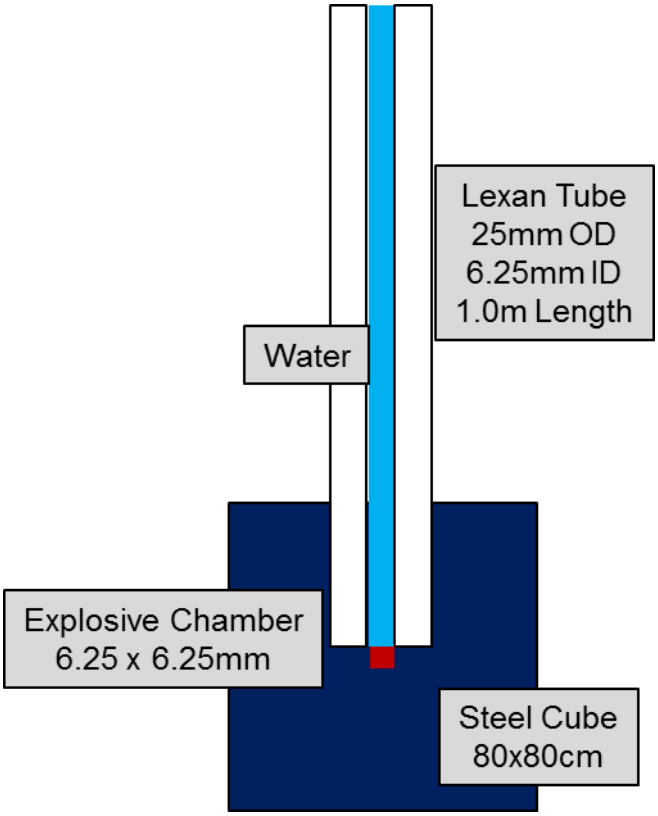

Figure 19 Schematic of Moby Dick test apparatus.

When the explosive is detonated, via a 50mg PETN exploding bridge wire, the interface between the detonation products and water is monitored via an electronic framing and streak cameras. The water column is ejected from the top of the Lexan tube and hence the name of a Moby Dick test; with apologies to Herman Melville.

A few notes about the test apparatus description:

- A search of Lexan suppliers did not indicate a stock tube of the dimensions described by Miller & Guirguis, i.e. 2.5cm OD with 0.625cm ID, or more likely, as the tests were conducted in the United States, 1 inch OD and 0.25 inch ID with a wall thickness of 3/8 inch.
- The indicated explosive chamber dimensions of 0.625cm diameter and 0.625cm height corresponds to a volume of $0.191 cm^3$. For the largest density explosive reported, i.e. aluminum (AL) combined with ammonium perchlorate (AP), of $1.88\ g/cm^3$ the mass of the explosive would be 0.36g. However, the introductory text provided by Miller & Guirguis states: "…small charges (as little as 1/2 gram) …". To accommodate 0.5 grams of AL/AP requires an explosive charge height of 0.9cm.
- For the two explosives types tested, i.e. Pentolite and AL/AP, Miller & Guirguis never explicitly state the amount of explosive used in each test. In this manuscript, it is assumed 0.5grams of explosive were used in both tests.

LS-DYNA Model of the Moby Dick Test

A simplified axisymmetric model of the Miller & Guirguis test apparatus was constructed by omitting both the Lexan tube and steel block. The water column and explosive charge were modeled using quadrilateral shell elements (axisymmetric solids) with appropriate zero velocity constraints at the outer radius and below the explosive charge. The primary model used the LS-DYNA Multi-Material Arbitrary Eulerian Lagrange (MM-ALE) solver. A corresponding Lagrange model was also used, as in 1993 Miller & Guirguis use of DYNA2D would only have had a Lagrange solver; it is possible they used the available 2D rezoning capability, but there is no mention of this, or any other mesh, i.e. mesh size, details of their DYNA2D model.

Two uniform mesh sizes of 0.5 and 0.25mm, were used to assess mesh convergence. Both mesh sizes produced essentially the same result, so the 0.5mm mesh, i.e. 6 elements across the radius of the charge, and tube, results are reported in this manuscript.

The Gruneisen equation-of-state was used for water with the following input parameters: density 0.001 g/mm^3, sound speed 1.48×10^3 mm/ms (or m/s), $S_1 = 1.92$, $S_2 = S_3 = 0$ and $\Gamma = 0.1$.

Miller & Guirguis in their Table 10, here preproducesd also as Table 10, provide the standard and time dependent JWL equation-of-state parameters for their two primary explosives:

Table 10 Miller & Guirguis provided JWL equation-of-state parameters.

Parameter	Pentolite	AL/AP Standard	AL/AP Time Dependent
A (Mbar)	5.3177	18.83	6.9513
B (Mbar)	0.0893	1.375	0.0313
R_1	4.6	8.0	5.4
R_2	1.05	4.0	1.4
ω	0.33	0.40	0.40
E_0 (Mbar)	0.08	0.095	0.07
a			0.0065
Q (Mbar)			0.110
P_{CJ} (Mbar)	0.235	0.150	0.150
D_{CJ} (mm/μs)	7.36	5.9	5.9
ρ_0 (g/cm^3)	1.65	1.88	1.88

Pentolite Results for Moby Dick Test

Figure 20 shows the Miller & Guirguis detonation products-and-water interface motion history, as hand digitized from their Figure 2. The black dots are the experimental measurements and the solid black line is the Miller & Guirguis DYNA2D simulation result using the standard JWL parameters provided in Table 10. The dashed and dotted lines are the present LS-DYNA JWL results for two mesh sizes. As can be seen, all the simulation results are in close agreement with

the measurements. Note: as mentioned above, a 0.5g Pentolite charge with diameter 6.25mm and height 10mm for the slightly lower density of Pentolite explosive was used in the LS-DYNA simulations.

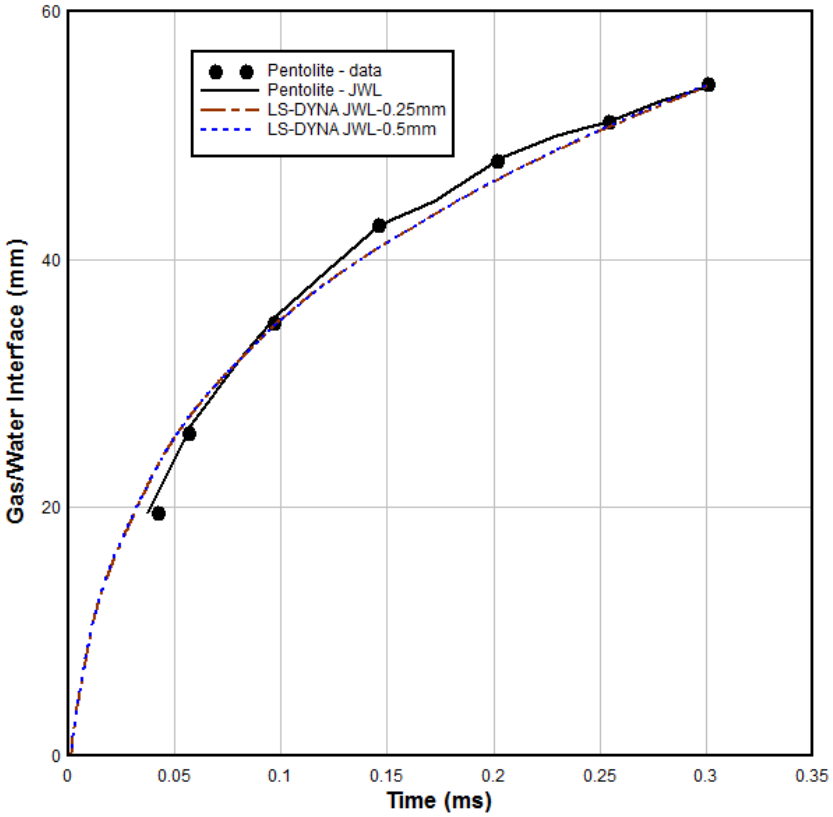

Figure 20 Comparison of Miller & Guirguis Pentolite experimental and simulation results.

AL/AP Results for Moby Dick Test

The good agreement between the data and simulation results for the Pentolite explosive provides some confidence that at least the standard JWL LS-DYNA simulation results should agree with the Miller & Guirguis standard JWL results from their Figure 20.

Standard JWL Parameter Simulation Results

Figure 21 shows the Miller & Guirguis standard JWL AL/AP interface motion history, i.e. black line. Included in this figure are the results from LS-DYNA for both a 0.5 and 0.75g charges. Neither LS-DYNA charge mass reproduces the Miller & Guirguis standard JWL result. While the larger 0.75g LS-DYNA charge does have the same interface position at 0.3ms as the Miller & Guirguis result, neither charge mass replicates the early time rapid interface motion.

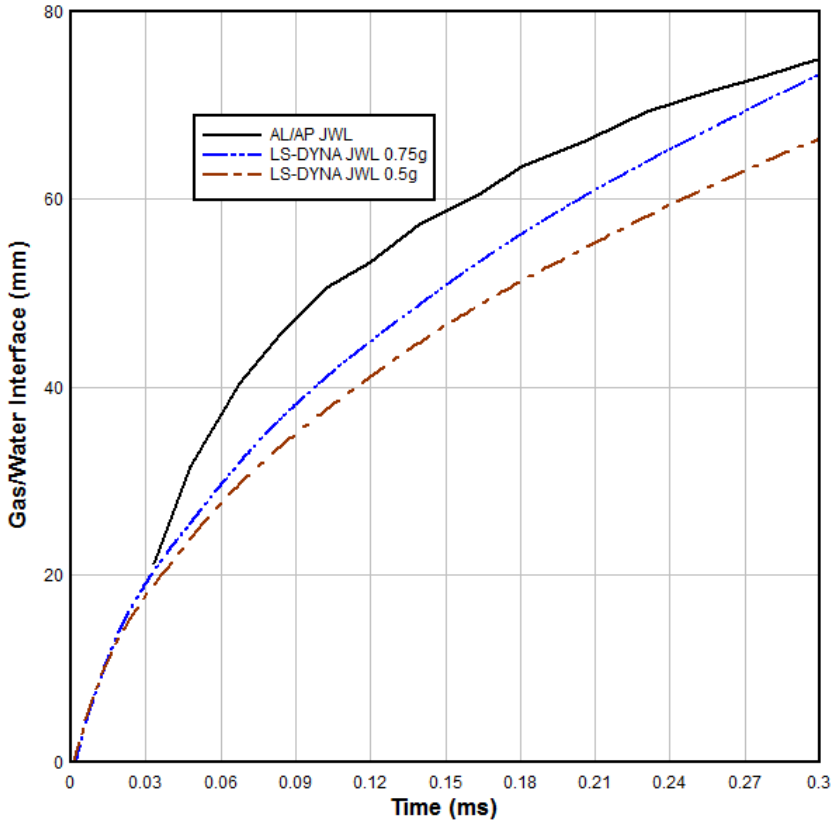

Figure 21 Comparison of Miller & Guirguis standard JWL result (black line) with the corresponding LS-DYNA results for two charge masses.

It is puzzling that the Pentolite simulation results for the standard JWL parameters agree well, but using the standard JWL parameters for AL/AP does not provide agreement with the corresponding Miller & Guirguis result. One speculation is the standard JWL parameters used by Miller & Guirguis are not the same as those listed in Table 10, e.g. a typographical error. Although the standard JWL parameters for Pentolite listed in Table 10 are similar to those provided by Dobratz & Crawford (1985), the reference cited by Miller & Guirguis for their standard JWL parameters is Kury et al. (1965), and not easily obtained reference.

Time Dependent JWL Parameter Simulation Results

Given that the present LS-DYNA standard JWL parameter results for AL/AP do not agree with the corresponding results presented by Miller & Guirguis, there is little hope the time dependent parameter results will agree. Still it may prove useful to other researchers to present time dependent results produced by LS-DYNA.

A time dependent Miller Extension option was added to the LS-DYNA standard JWL equation-of-state. Briefly, this modification involves adding an additional energy term λQ to the standard JWL equation-of-state. Here Q is the total afterburning energy to be added and λ is the time dependent fraction of the additional energy.

$$p = A\left(1-\frac{\omega}{R_1 V}\right)e^{-R_1 V} + B\left(1-\frac{\omega}{R_2 V}\right)e^{-R_2 V} + \frac{\omega\left(E+\lambda Q\right)}{V}$$

The rate expression for λ provided by Miller & Guirguis is

$$\frac{d\lambda}{dt} = a\left(1-\lambda\right)^{1/2} P^{1/6}$$

The two power coefficients in the above equation are sometimes generalized inputs, as in the present, and AUTODYN's, implementation of the Miller Extension.

Although the coefficient a is presented in Table 10 as dimensionless, for λ to be a dimensionless fraction between zero and unity, the coefficient a must have units of pressure to the -1/6 per unit time, e.g. the units for a in Table 10 should read

$$a = 0.0065/\left(\mu s - \text{Mbar}^{1/6}\right)$$

Users of Miller's Extension, in any implementation, should take heed of these units and realize that calibration of the parameter a, and the power coefficients, are dependent on the system of units used in the calibration process.

The LS-DYNA implementation of Miller's Extension includes a pressure conversion factor such that the Miller parameters provided in Table 10, or other literature citations, can be used with the user selected system of units. For example, assuming the user units for pressure is MPa, the pressure conversion factor, $\text{CONP} = 10^5$, is implemented for the pressure term in the rate equation as

$$\frac{d\lambda}{dt} = a\left(1-\lambda\right)^{1/2}\left(\text{CONP}\times P\right)^{1/6}$$

So the resulting converted pressure term has units of Mbar.

Because Miller & Guirguis did not provide time units for the parameter a, there are two likely possibilities:

$$a = 0.0065\ \mu\text{s}^{-1} = 6.5\ \text{ms}^{-1}$$
$$a = 0.0065\ \text{ms}^{-1}$$

Figure 22 illustrates the computed detonation products-water interface position for two values of the a parameter. The system of units used in the calculations was grams, millimeters, and milliseconds. The upper curve uses the Table 10 time unit converted value $a = 6.5/\text{ms}$ while the lower curve used the value as given in Table 10 without time unit conversion, i.e. $a = 0.0065/\text{ms}$.

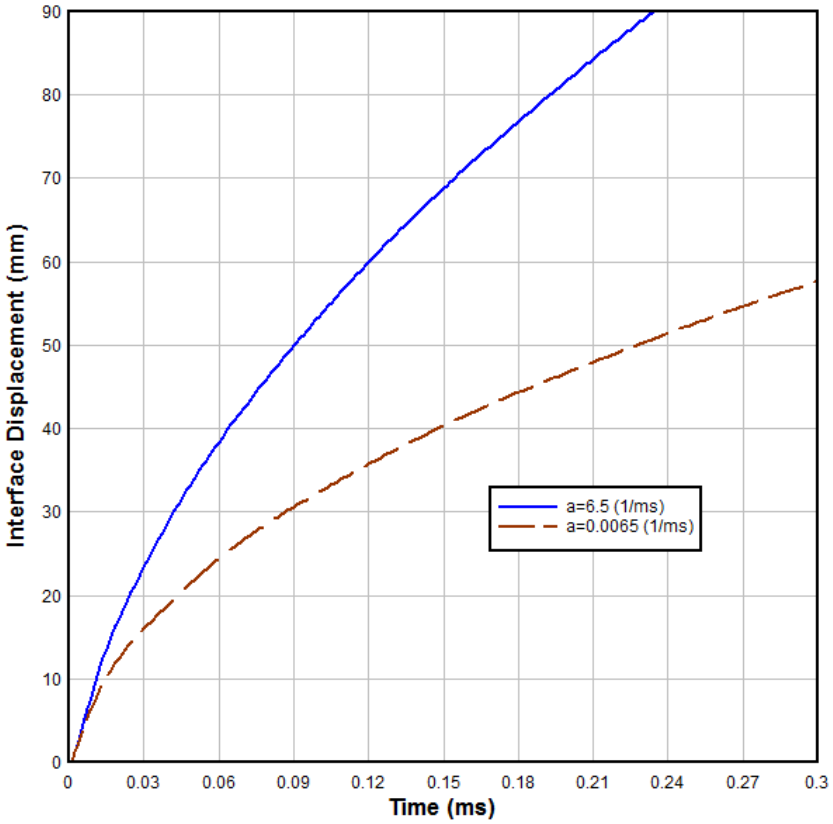

Figure 22 Effect of time units on Miller's a parameter.

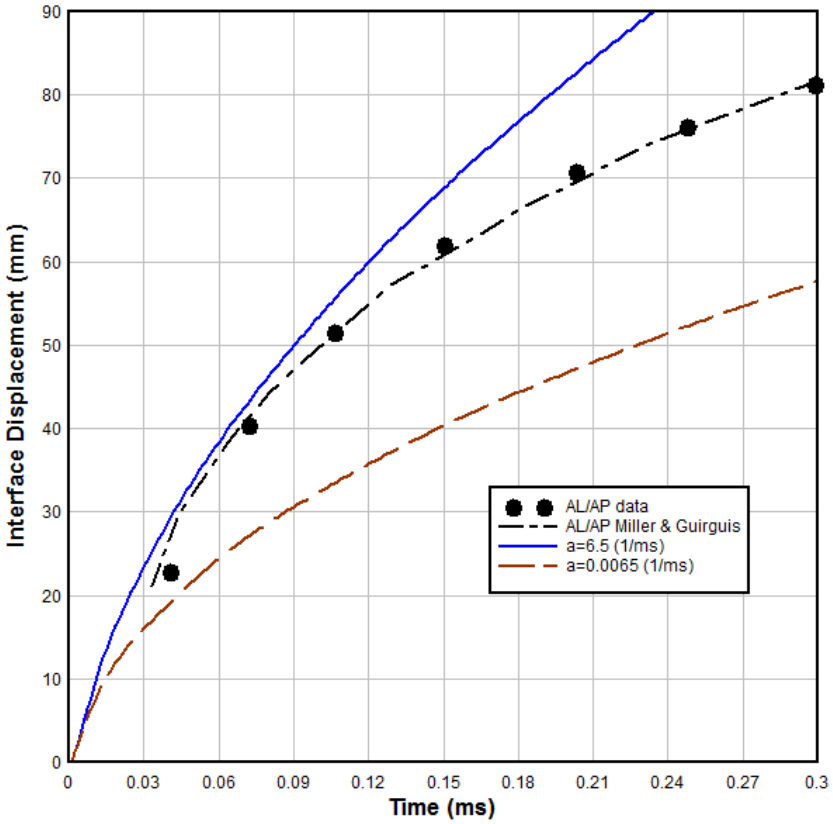

Figure 23 Comparison of the AL/AP interface data with the Miller & Guirguis simulation and corresponding LS-DYNA results.

Figure 23 compares the detonation products-water interface motion history for the data with the Miller & Guirguis simulation and the corresponding LS-DYNA simulation results. It should be noted that the close agreement of the Miller & Guirguis simulation results with the data is due to their using the data to calibrate the a and Q parameters provided in Table 10. The LS-DYNA result, with the time unit corrected $a = 6.5\ \mathrm{ms}^{-1}$ parameter (solid curve), is close to the initial data points, but significantly over estimates the displacement history.

A cubic polynomial was fit to the AL/AP displacement history data; with the point (0,0) added to the data. The time derivative of this displacement history provides the velocity history, which is compared to the corresponding LS-DYNA velocity history in Figure 24. The LS-DYNA velocity history is tending to a constant value of about 190m/s while the AL/AP data suggests the possibility the velocity might increase beyond 0.3ms.

The somewhat favorable comparison of the LS-DYNA result with the data is a bit surprising as the standard JWL AL/AP comparison to the Miller & Guirguis simulation with the corresponding LS-DYNA result, refer back to Figure 21, did not show good agreement. This again possibly indicates some difference between the AL/AP standard JWL equation-of-state parameters and those used by Miller & Guirguis.

At this point it is also worth mentioning that it is likely no two implementation of the Jones Wilken Lee equation of state should be assumed to be identical, until verified as being identical.

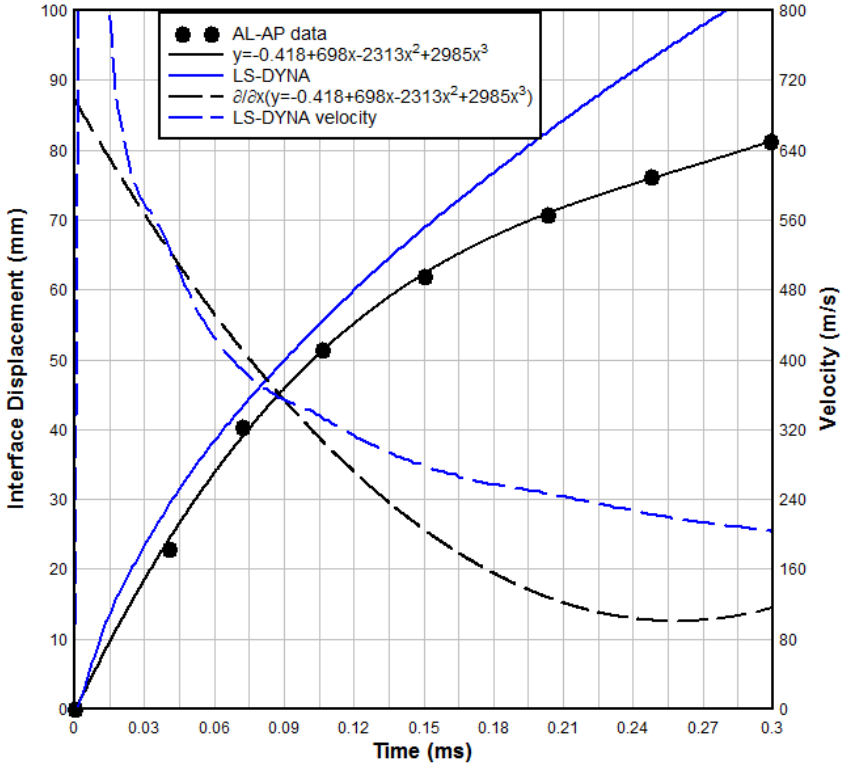

Figure 24 Comparison of interface displacement and velocity for the AL/AP data and the LS-DYNA Miller Extension model.

Acknowledgements

The author is grateful, and indebted, to Idan Edri of the Technion for his many helpful comments and cooperation in sharing his AUTODYN results. Special thanks to Dr. Nicolas Aquelet and Dr. Ushnish Basu of Livermore Software Technology Corporation for their help and guidance in navigating the addition of this afterburning equation of state to LS-DYNA. Initial AUTODYN comparative results were generously provided by Dr. Song Woei LIANG of the Singapore Ministry of Home Affairs. Gratitude is expressed to Mr. Bence Gerber and Dr. Chris Quan of ANSYS for responding to several questions regarding the AUTODYN documentation for afterburning, and to Dr. Lee Tarver of LLNL for his helpful comments and provision of key references.

References

Birnbaum, N.K., G.E. Fairlie and N.J. Francis, (1998), "Numerical Modeling of Small Scale Water Mitigation Feasibility Tests," Century Dynamics, Incorporated, Technical Report to the Naval Facilities Engineering Service Center, Port Hueneme, California under Contract No: N47408-97-M-0928

Dobratz B.M. and Crawford P.C., "LLNL Explosives Handbook - Properties of Chemical Explosives and Explosive Stimulants," Lawrence Livermore National Laboratory, UCRL-52997, January 1985.

Fried L.E., W.M. Howard and P.C. Souers, (1998) "Cheetah 2.0 User's Manual," Lawrence Livermore National Laboratory, Livermore, CA, 1998

Edri1, J., V.R. Feldgun, Y.S. Karinski and D.Z. Yankelevsky (2012) "On Blast Pressure Analysis Due to a Partially Confined Explosion: III. Afterburning Effect," *International Journal of Protective Structures*, Volume 3, Number 3, pages 311-331.

Edri, I., Feldgun, V. R., Karinski, Y. S. & Yankelevsky, D. Z., (2013) "Afterburning Aspects in an Internal TNT Explosion," *International Journal of Protective Structures*, Volume 4, Number 1, pp. 97-116.

Keenan, W.A. and P.C. Wager, (1992), "Mitigation of Confined Explosion Effects by Placing Water in Proximity of Explosives," 25th DoD Explosives Safety Seminar, Anaheim, CA, 18–20 August.

Kuhl A. L, Forbes J., Chaudler J., Oppenheim A. K, Spektor R., Ferguson R.E. (1998). "Confined combustion of TNT explosion products in air," Lawrence Livermore National Laboratory Report UCRL-JC-131748, Livermore, CA

Kuhl A.L., M. Howard and L. Fried (2003) "Thermodynamic model of afterburning in explosions," *34th Intl. ICT Conference: Energetic Materials: Reactions of Propellants, Explosives, and Pyrotechnics*, Karlsruhe, Germany.

Kury, J.W., H.C. Hornig, E.L. Lee, J.L. McDonnel, D.L. Ornellas, M. Finger, F.M. Strange, and M.L. Wilkins, "Metal Acceleration of Chemical Explosives," Fourth (International) Symposium on Detonation, ACR-126 (1965).

Lee, E.L., M. Finger, and W. Collins, (1998), "JWL Equation of State for High Explosives," Lawrence Livermore Laboratories, UCID-16189, University of California, Livermore, CA.

Miller, P.J. (1996) "A Reactive Flow Model with Coupled reaction Kinetics for Detonation and Combustion of non-ideal explosives," *Materials Research Society Symposium Proceedings,* Volume 418, pages. 413-419, Materials Research Society Publication

Miller, P.J. and R.H. Guirguis, "Experimental Study and Model Calculations of Metal Combustion in AL/AP Underwater Explosives," Proceedings of 1993 Material Research Society (MRS) meeting (MRS, Pittsburgh, Pennsylvania, 1993), Volume 296, Pages 299-303.

POON, J.K, R. CHAN and D. CHNG, (2014) "Sensitivity of JWL Parameters in Air Blast Modelling," Presented at the 23rd Military Aspects of Blast (MABS), Oxford UK.

Souers P.C. and L.C. Haselman Jr., (1993) "Detonation Equation of State at LLNL," Lawrence Livermore National Lab., CA, UCRL-ID—116113.

Souers P.C. B. Wu and L.C. Haselman Jr., (1995) "Detonation Equation of State at LLNL," Lawrence Livermore National Labortory, CA UCRL-ID--119262-Rev.3.

Appendix – Afterburning Models

This appendix provides brief descriptions of the afterburning models used in the main body of this text.

AUTODYN & LS-DYNA Simple Afterburn Algorithm

Referred to in the AUTODYN new feature Version 11.0 document as the "Time Dependant (sic) Energy Deposition Extension to JWL Equation of State," this algorithm has three input parameters: the amount of afterburn energy to be added and the start and end times for adding the energy.

The JWL equation of state is modified by the afterburning energy term Q added over time to the standard internal energy per unit volume, E, viz.

$$p = A\left(1-\frac{\omega}{R_1 V}\right)e^{-R_1 V} + B\left(1-\frac{\omega}{R_2 V}\right)e^{-R_2 V} + \frac{\omega\left(E+Q\right)}{V}$$

For TNT, three references are cited by Edri et al. (2013) for determining the total amount of afterburning energy when there is complete combustion of the detonation products. For partial combustion, they present a calculation of the total energy release based on the ratio of the charge mass to the available volume of air. Determining the time to start and end the addition of the afterburn energy is a more subjective. In Edri et al (2012) the following practical suggestion is made:

> "T0 is defined as the time at which the first shock wave reflects from the nearest wall and interacts with the detonation products. T1 is defined as the time at which the temperature is lower than the average ignition temperature and beyond this time the afterburning is not possible."

Left unsaid in the AUTODYN documentation is how the afterburn energy is add over this time period, i.e. at a constant rate or linearly increasing rate.

Pressure Shift Afterburn Approximation

In Edri et al (2013) the following approximation of the afterburn pressure history is provided as their Equation (9)

$$P(t)_{\text{shifted}} = P(t)_{\text{No-Afterburn}} + P_{\text{final}}\left(K_{\text{ab}}-1\right)$$

where $P(t)_{\text{shifted}}$ is the approximation of the afterburn pressure history obtained by shifting the non-afterburn pressure history $P(t)_{\text{No-Afterburn}}$ with the addition of the constant pressure comprised of the final pressure P_{final} from the non-afterburn simulation multiplied by the afterburn energy scaling factor $\left(K_{\text{ab}}-1\right)$. The parameter K_{ab}, termed the afterburning ratio, is the ratio of the total energy released to the detonation energy, and is a function of the charge mass to the volume of available air; see Figure 4 in Edri et al. (2013). For TNT the afterburn coefficient varies from about 3.3 to unity between mass-to-volume ratios of 0.386 to 50kg/m^3, respectively. A ratio of 1.87kg/m^3, represents the lowest mass-to-volume ratio allowing for full afterburning.

The above shifted pressure history can be further simplified by again noting the final pressure can be estimate as the final impulse divided by the duration. Thus integrating the above equation over time and noting

$$P_{\text{final}} \approx \int P_{\text{No-Afterburn}}\,dt$$

Then

$$P_{\text{Afterburn}} = K_{ab} P_{\text{final}}$$

Thus an estimate of the final afterburn pressure can easily be obtained from the simulation result without afterburning.

Appendix – JWL Parameters for TNT

This collection of TNT JWL parameters was provided by Poon et al. (2014)

JWL Parameter	Lee et al. (1973)	Dobratz & Crawford (1985)	Souers & Hasselman (1993)	Souers, Wu & Hasselman (1995)
A (GPa)	373.75	371.25	524.41	454.86
B (GPa)	3.747	3.231	4.90	10.119
R_1	4.15	4.15	4.579	4.5
R_2	0.90	0.95	0.86	1.5
ω	0.35	0.30	0.23	0.25
E_0 (GPa)	6.0	7.0	7.1	7.8